# REPORT 999

# INVESTIGATION OF THE NACA 4-(3)(08)-03 AND NACA 4-(3)(08)-045 TWO-BLADE PROPELLERS AT FORWARD MACH NUMBERS TO 0.725 TO DETERMINE THE EFFECTS OF COMPRESSIBILITY AND SOLIDITY ON PERFORMANCE[1]

By JOHN STACK, EUGENE C. DRALEY, JAMES B. DELANO, and LEWIS FELDMAN


## SUMMARY

*As part of a general investigation of propellers at high forward speeds, tests of two 2-blade propellers having the NACA 4-(3)(08)-03 and NACA 4-(3)(08)-045 blade designs have been made in the Langley 8-foot high-speed tunnel through a range of blade angle from 20° to 60° for forward Mach numbers from 0.165 to 0.725 to establish in detail the changes in propeller characteristics due to compressibility effects. These propellers differed primarily only in blade solidity, one propeller having 50 percent more solidity than the other.*

*Serious losses in propeller efficiency were found as the propeller tip Mach number exceeded 0.91, irrespective of forward speed or blade angle. The magnitude of the efficiency losses varied from 9 percent to 22 percent per 0.1 increase in tip Mach number above the critical value. The range of advance ratio for peak efficiency decreased markedly with increase of forward speed. The general form of the changes in thrust and power coefficients was found to be similar to the changes in airfoil lift coefficient with changes in Mach number. Efficiency losses due to compressibility effects decreased with increase of blade width. The results indicated that the high level of propeller efficiency obtained at low speeds could be maintained to forward sea-level speeds exceeding 500 miles per hour.*


## INTRODUCTION

Limitations of the screw propeller as a propulsive element for aircraft due to adverse compressibility effects have been recognized for several years. Airfoil and propeller investigations have shown that marked decreases in propeller efficiency are encountered as blade-section speeds approach the speed of sound. Some existing information has been interpreted as showing that screw propellers might become impracticable because of compressibility losses at speeds slightly higher than current blade-section speeds. Other information has been interpreted as contradictory of this conclusion. Two deductions that appear to be clear are: First, the true magnitude of the losses is relatively unknown and, second, the losses are of magnitude sufficient to require considerable research leading to the development of improved propellers if current efficiencies are to be maintained.

Available airfoil data are essentially two-dimensional and when applied without correction for three-dimensional effects, as at a tip, and without correction for tunnel-wall effects, which at high Mach numbers are still uncertain, may give unduly pessimistic results. On the other hand, existing propeller data obtained at high tip speeds but low forward speeds are nonconservative when applied to computations for high forward speeds because the variation of Mach number along the blade is incorrect. Propeller efficiency at high forward speed estimated by the use of these data is too high. Some flight test data have been obtained by various experiments which show critical tip Mach numbers of 0.88 to 1.0. Some of these results are questionable because of the practical impossibility of obtaining adequately controlled test conditions. Furthermore, none of the flight data permit an evaluation of the compressibility losses because the blade-section speeds are in the compressibility range even for the lowest speeds investigated.

Several years ago the NACA, recognizing the seriousness of the problem, instituted a long-range research program to lead to the development of improved propellers at high forward speeds. Early phases of this work were airfoil studies that led to the design of sections having high critical Mach numbers (reference 1). Existing propeller dynamometers were unsuitable because of inadequate power for this extensive research, and the building of new and adequately powered dynamometers was also undertaken. Shortly after this program was instituted, the defense program and later the war emergency arose and many delays in the procurement of blades and equipment were encountered because of priorities assigned to other work. Recognizing the need for propeller development and for study of compressibility phenomena as related to propellers, the Langley Laboratory proposed an emergency investigation with immediately available equipment to study particularly the compressibility phenomena.

The present research consists of investigations of two-blade propellers over an extensive range of Mach number and blade angle and includes, in addition to the effects of compressibility, the effects of solidity and blade-section camber. The first results of this investigation which are

[1] This report contains material originally issued as NACA ACR 4A10 and ACR 4B16 in January and February 1944, which until recently have been subject to security regulations.

related to the effects of compressibility and solidity on propeller performance are presented in this report for two propellers having late-critical-speed blade sections and differing essentially only in solidity. One propeller has conventional solidity and the other propeller has 50 percent greater design solidity.

## SYMBOLS

| | |
|---|---|
| $b$ | blade width, feet |
| $c_{l_d}$ | blade-section design lift coefficient |
| $C_P$ | power coefficient $\left(\frac{P}{\rho n^3 D^5}\right)$ |
| $C_T$ | thrust coefficient $\left(\frac{T}{\rho n^2 D^4}\right)$ |
| $D$ | propeller diameter, feet |
| $b/D$ | blade width ratio |
| $h$ | maximum thickness of blade section, feet |
| $h/b$ | blade thickness ratio |
| $J$ | advance ratio $(V_0/nD)$ |
| $M$ | tunnel-datum (forward) Mach number (tunnel-empty Mach number uncorrected for tunnel-wall constraint) |
| $M_t$ | helical tip Mach number $\left(M\sqrt{1+\left(\frac{\pi}{J}\right)^2}\right)$ |
| $M_{t_{cr}}$ | critical tip Mach number |
| $n$ | propeller rotational speed, revolutions per second |
| $P$ | power absorbed by the propeller, foot-pounds per second |
| $P_c$ | power disk-loading coefficient $\left(\frac{P}{\frac{1}{2}\rho V_0^3 S}\right)$ |
| $R$ | propeller tip radius, feet |
| $r$ | blade-section radius, feet |
| $S$ | propeller disk area, square feet $\left(\frac{\pi D^2}{4}\right)$ |
| $T$ | propulsive thrust of propeller, pounds |
| $T_c$ | thrust disk-loading coefficient $\left(\frac{T}{\rho V^2 D^2}\right)$ |
| $V$ | tunnel-datum velocity (tunnel-empty velocity uncorrected for tunnel-wall constraint), feet per second |
| $V_0$ | equivalent free-air velocity (tunnel-datum velocity corrected for tunnel-wall constraint), feet per second |
| $r/R$ | blade-section station |
| $\beta$ | section blade angle, degrees |
| $\beta_{0.75R}$ | section blade angle at 0.75 tip radius, degrees |
| $\eta$ | propulsive efficiency $\left(\frac{C_T}{C_P}J\right)$ |
| $\eta_i$ | maximum propulsive efficiency at low tip Mach number $(M_t \approx 0.25)$ |
| $\eta_{max}/\eta_i$ | relative maximum efficiency |
| $\eta_{max}$ | maximum propulsive efficiency |
| $\rho$ | air density, slugs per cubic foot |

## APPARATUS AND METHODS

The investigation was conducted in the Langley 8-foot high-speed tunnel. The propeller-model configuration investigated is shown in figure 1.

**Propellers.**—Two 2-blade propellers were used in this investigation. These propellers are designated as the NACA 4-(3)(08)-03 and the NACA 4-(3)(08)-045 blade designs. The designation numbers describe the propellers. The number (or numbers) of the first group is the diameter in feet; the number (or numbers) of the second group (enclosed within the first set of parentheses) is the design lift coefficient (in tenths) of the blade section at the 0.7-radius station; the numbers of the third group (enclosed within the second set of parentheses) are the thickness ratio of the blade section at the 0.7-radius station; and the numbers of the fourth group are the blade solidity expressed as the ratio of the blade chord at the 0.7-radius station to the circumference of the circle having a radius 0.7 of the propeller tip radius. The NACA 4-(3)(08)-045 propeller thus has a diameter of 4 feet and the blade section at the 0.7-radius station has a design lift coefficient of 0.3, a thickness ratio of 0.08, and a blade solidity of 0.045.

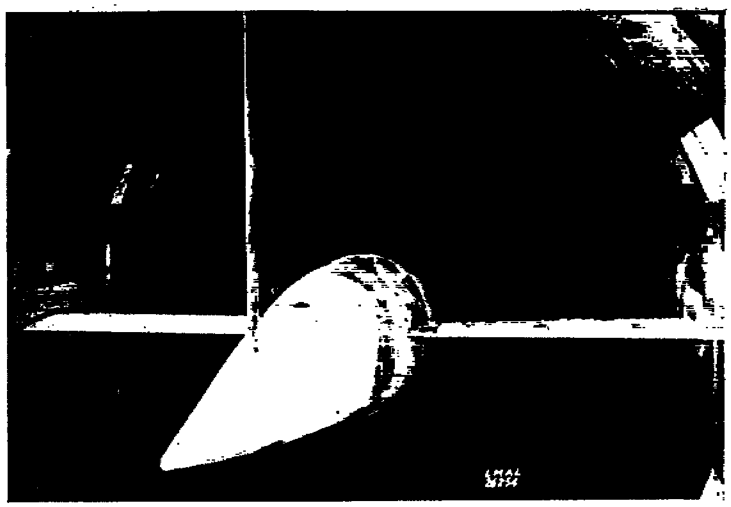

(a) Wing-fuselage model.

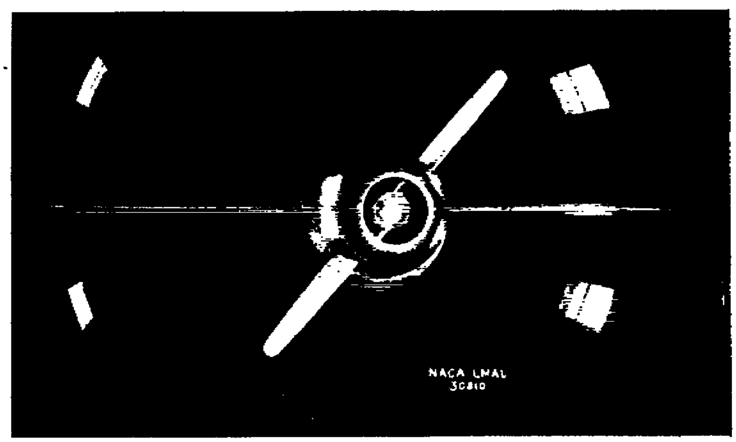


(b) NACA 4-(3)(08)-03 propeller installation.

FIGURE 1.—Installation for propeller investigation in Langley 8-foot high-speed tunnel.

The propellers were originally designed and constructed for use in an extensive and general investigation of propellers at high forward Mach numbers. The blades of these propellers were designed for a three-blade propeller to produce minimum induced energy losses (profile drag assumed equal to zero) at a blade angle of approximately 45° at the 0.7-radius station. The blade sections are late-critical-speed sections of the NACA 16 series (reference 1); methods and principles employed in the design of the blades are discussed in reference 2. The blades differ primarily only in blade width. (The NACA 4-(3)(08)-03 blade is of conventional width.) Blade-form curves for the propellers tested are presented in figure 2.

The blades were made of duralumin and were constructed in the Langley shops. The blade sections and other general dimensions were accurate within 0.002 inch. A photograph of the blades is shown as figure 3.

**Wing-fuselage model.**—The model (fig. 1) was especially designed to have a high critical Mach number. The NACA E cowling, which was designed for high critical Mach number from basic studies of air inlets in a streamline body (reference 3), was used. This particular cowling was originally tested in a general study of pursuit-airplane performance (reference 4). The wing of the model extended through the tunnel walls and was fastened to the balance system. The airfoil section was a modified NACA 66-series section of 9 percent thickness and 20-inch chord. The critical Mach number of the model exceeded 0.75. The highest forward Mach number at which these investigations were conducted was 0.74. In some of the preliminary runs, excessive vibration of the model was encountered at some speeds and was eliminated by a vertical streamline support that secured the tail of the model to the balance ring outside the tunnel. This support had a critical Mach number of 0.80.

The propeller hub was contained within the inner spinner of the cowling and the portions of the blade between the inner and outer cowlings were shielded from the air flow by cuffs secured to the spinner (figs. 1 and 4). The outside diameter of the cowling at the propeller plane was one-third of the propeller diameter; hence, only the blade sections having good aerodynamic form were exposed to the air stream.

There was a small gap between the propeller and the outer spinner at the station where the blades projected through the spinner. This gap was sealed by a strip of sponge rubber cemented to the blades (fig. 4) to prevent radial outflow from the cowling.

**Dynamometer.**—The dynamometer was completely enclosed by the fuselage. Dynamometer details are shown in figure 5. The motor was 10 inches in diameter and 30 inches long. It was rated at 200 horsepower at 4,900 rpm for ½ hour of

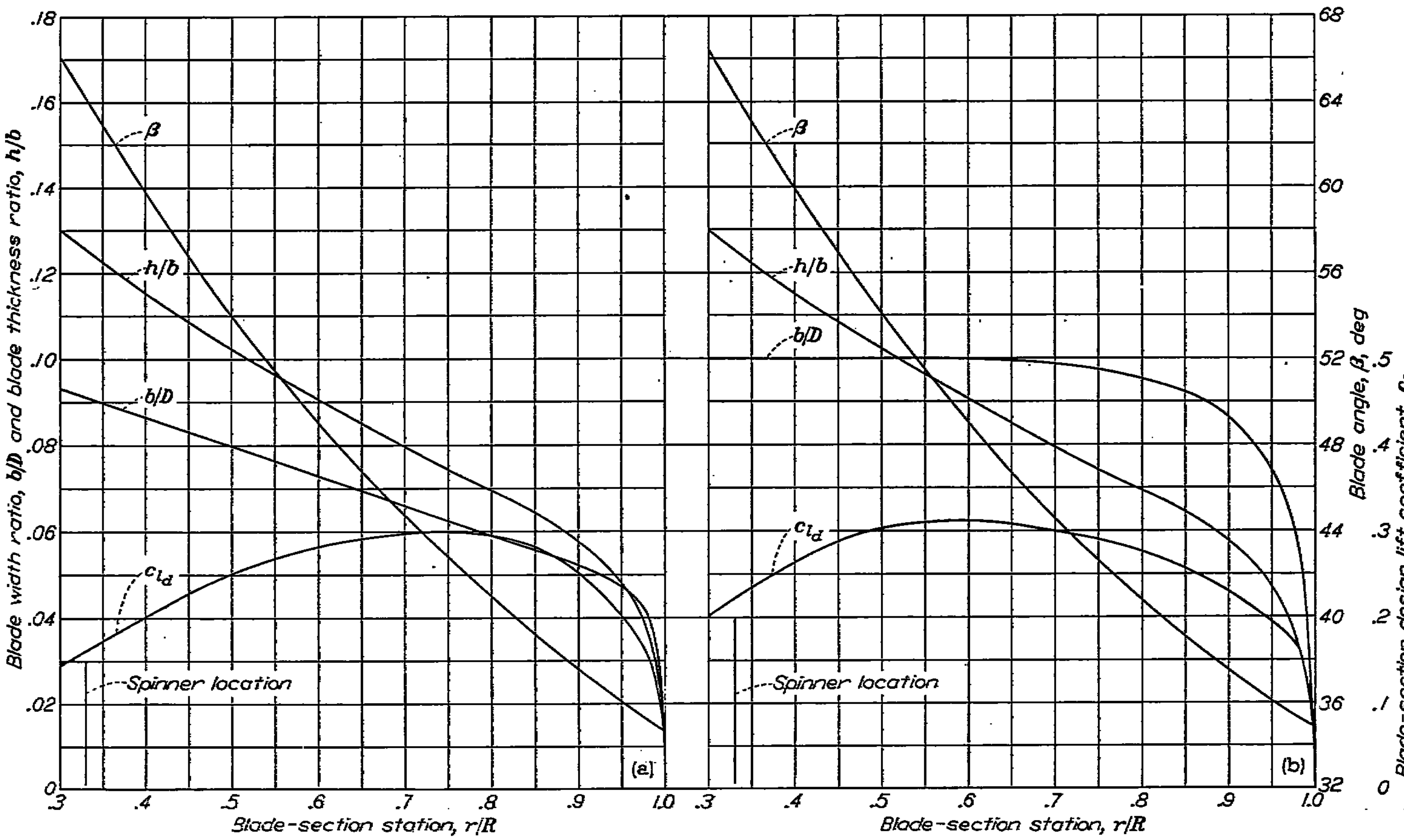

(a) NACA 4-(3)(08)-03 propeller.
(b) NACA 4-(3)(08)-045 propeller.

FIGURE 2.—Blade-form curves.

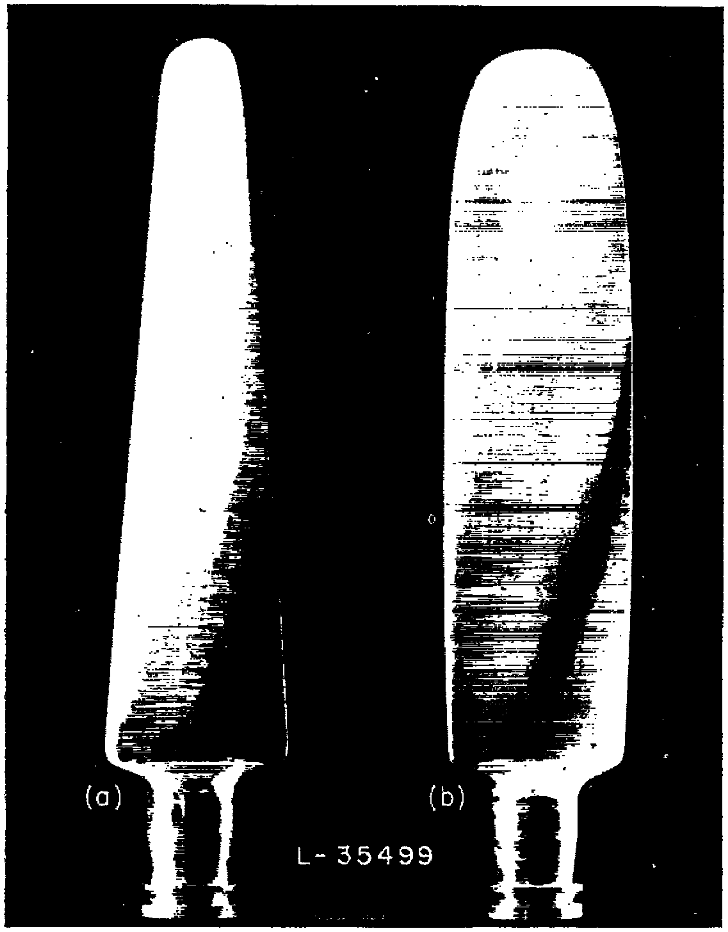


(a) NACA 4-(3)(08)-03. (b) NACA 4-(3)(08)-045.
FIGURE 3.—Blade designs investigated.

operation. Some of the runs were limited because of lack of power even though a considerable overload above the normal ½-hour rating was employed. Continuous speed control of the induction motor was obtained by the use of a variable-frequency power supply.

The motor housing was mounted on bearings coaxial with the shaft and was held from rotating under the torque reaction by a cantilever spring. One end of this cantilever spring was rigidly fixed to the frame of the model and the other end was held in contact with the motor casing through torque reaction. The contact between spring and motor casing was through roller bearings in the end of the spring and bearing plates fastened to the motor casing.

The propeller torque is the motor torque reaction acting on the cantilever spring. This torque was measured by electrical strain gages cemented to the cantilever spring. Four strain gages were used to form the arms of a Wheatstone bridge. By arranging two gages on each side of the spring, it was possible to provide temperature-effect compensation and to obtain adequate sensitivity. For runs at low values of torque, a similar but weaker spring was used to obtain improved accuracy. A photograph of the springs with strain gages installed is shown as figure 6.

The strain gages were calibrated by applying known weights at the end of an arm fastened to the motor casing and by recording the bridge unbalance as the torque. Linear calibrations were obtained in which the measured torque values were within $\pm 0.5$ percent of the applied values.

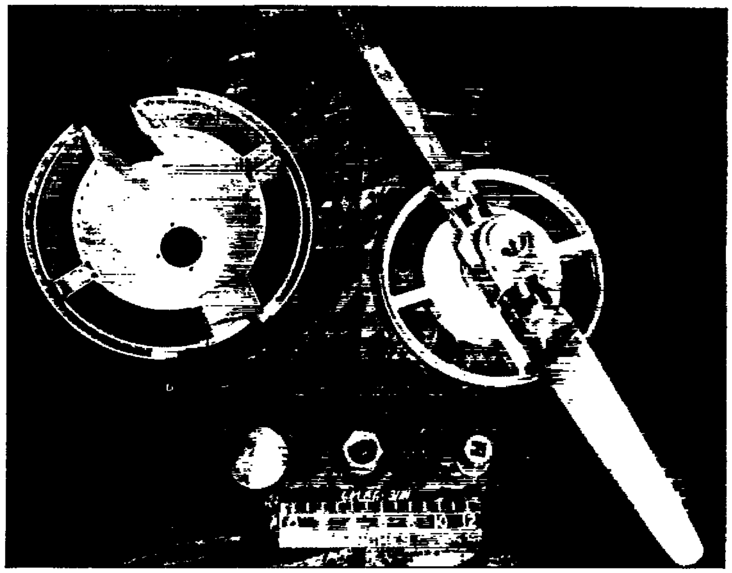

FIGURE 4.—Propeller hub and spinner.

**Thrust balance.**—The thrust was measured by the tunnel drag balance. The force indicated by the drag balance was the resultant force along the thrust axis, that is, the thrust of the propeller minus the drag of the model. The propulsive thrust was determined as the resultant force in the thrust direction minus the drag of the model without the propeller. The variation in body drag due to variation in aerodynamic smoothness from run to run was determined from many repeat tests of the body without the propeller and was found to be less than $\pm 1$ percent of the value of the propulsive thrust at maximum efficiency.

**Rotational speed.**—The propeller rotational speed was measured by a condenser-type tachometer attached to the motor shaft. A check on the accuracy of this instrument was provided by comparing its readings with those obtained from known Lissajous' figures on an oscilloscope connected to an alternator on the motor shaft. Generally, the rotational speeds obtained from both instruments agreed to within $\pm 3$ rpm.

## TESTS

Thrust, torque, and rotational speed were measured throughout the operating range of the propellers. The range of blade angle covered for each test Mach number is given in table I.

TABLE I.—TEST RANGE OF BLADE ANGLE AND MACH NUMBER

| Tunnel-datum (forward) Mach number | Blade angle at 0.75 radius, $\beta_{0.75R}$ (deg) | | | | | | | | |
|---|---|---|---|---|---|---|---|---|---|
| 0.165 | 20 | 25 | 30 | 35 | 40 | 45 | 50 | 55 | 60 |
| .23 | [a]20 | 25 | 30 | 35 | 40 | 45 | 50 | 55 | 60 |
| .35 | — | — | 30 | 35 | 40 | 45 | 50 | 55 | 60 |
| .43 | — | — | — | 35 | 40 | 45 | 50 | 55 | 60 |
| .53 | — | — | — | — | 40 | 45 | 50 | 55 | 60 |
| .60 | — | — | — | — | — | 45 | 50 | 55 | 60 |
| .65 | — | — | — | — | — | — | 50 | 55 | 60 |
| .675 | — | — | — | — | — | — | 50 | 55 | 60 |
| .70 | — | — | — | — | — | — | 50 | 55 | 60 |
| .725 | — | — | — | — | — | — | [a]50 | [a]55 | [a]60 |

[a] Not tested for the NACA 4-(3)(08)-045 propeller.

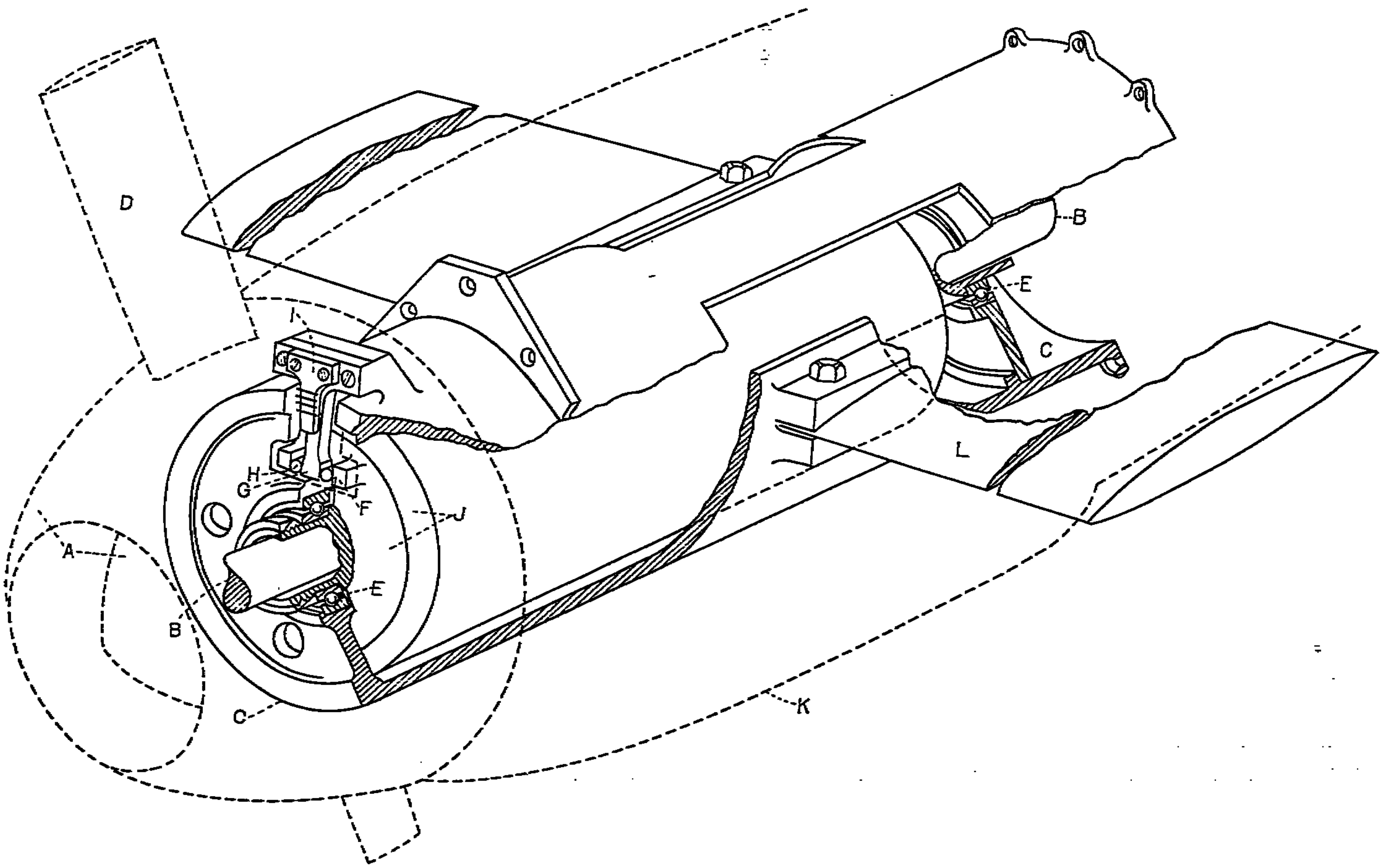


A Spinner (see fig. 1 (b))
B Motor shaft
C Main housing
D Propeller
E Ball bearing
F Hardened bearing plate
G Torque spring (see fig. 6)
H Hardened roller
I Terminal block for strain gage
J Motor casing
K Fuselage
L Wing

FIGURE 5.—Dynamometer details.

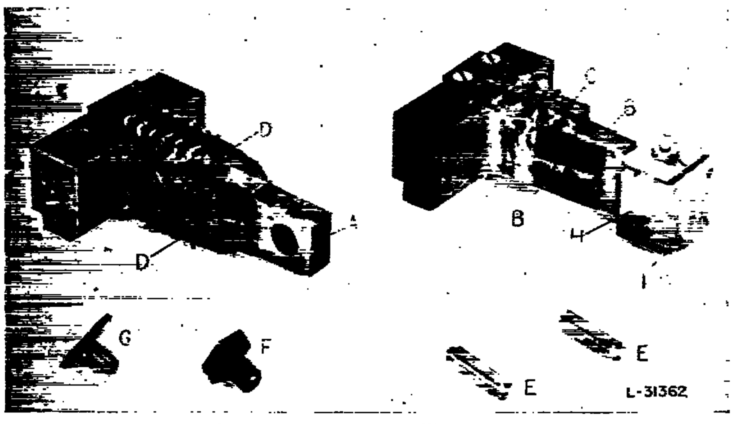


A Spring
B Strain gages
C Terminal block
D Felt insulation
E Hardened roller
F Bearing plate
G Bearing plate
H Bearing plate
I Roller retainer

FIGURE 6.—Cantilever springs with strain gages.

The test procedure consisted in setting the blade angle at the desired value and raising the tunnel airspeed to the desired tunnel-datum Mach number with the propeller windmilling. The range of advance ratio was then covered by increasing the propeller rotational speed while the tunnel-datum Mach number was held constant. The ranges of advance ratio and tunnel-datum Mach number were limited by either one of two factors, the propeller rotational speed or the power of the propeller drive motor. For the low blade angles, the propeller-rotational-speed limit of 5,000 rpm was the principal restriction and, for the high blade angles, power limitation of the motor was the principal restriction. The data obtained, however, are adequate for determination of maximum efficiencies and the shape of the propeller-efficiency curve for the advance ratios required for zero thrust to advance ratios less than those required for maximum efficiency. The normal operating range of Mach number and advance ratio for each blade angle thus was covered.

## REDUCTION OF DATA

The data have been reduced to the usual thrust and power coefficients and efficiency and have been corrected for the propulsive effects of the cowling and spinner and for tunnel-wall constraint. The tunnel-wall constraint necessitated a velocity correction to free-air conditions and a model-drag correction because of the buoyancy effect.

**Thrust.**—The thrust coefficient was determined from the propulsive thrust. The force actually measured during the propeller tests was the net force in the drag direction. The thrust was then determined as the net measured force minus the drag of the model without the propeller and minus the thrust due to the buoyancy effect. The model was so mounted that a lift coefficient of approximately 0.1 was attained at the highest forward speeds. The thrust axis was therefore inclined at a small angle, slightly less than 1° to the direction in which the drag force was measured by the balance. The cosine correction, however, is insignificant and therefore has not been applied.

**Power.**—The power coefficient was determined from the readings of the calibrated strain gages. Some difficulty was encountered with the strain-gage operation and frequent calibrations were made. When changes in calibration were found, repeat tests of the propeller were always made.

**Nose-blower thrust and power.**—The nose-blower cowling contributed both thrust and torque to the measured thrusts and torques. The cuffs, which shielded the propeller shanks within the cowling, acted as blower blades and were designed to operate at appreciable values of lift coefficient in the low advance-ratio range and gradually to approach operation at zero lift coefficient in the high advance-ratio range. The propeller thrust and torque coefficients have been corrected for the effect of the blower. These corrections were determined from tests of the blower alone operated through a wide range of advance ratio at each test Mach number. The results of these data were reduced to thrust and power coefficients.

**Velocity correction due to tunnel-wall constraint.**—Owing to the constraint of the tunnel walls, the equivalent free-stream velocity corresponding to the thrust and torque of the propeller measured at each rotational speed differs from the tunnel-datum velocity (tunnel empty). The correction to the tunnel-datum velocity was evaluated by surveys of the total and static pressures in three planes: 12 inches in front of and 3 and 12 inches behind the plane of the propeller. These surveys extended radially from the tunnel wall to the tip location of the propeller. The velocity correction was then evaluated by the method of reference 5. This correction, which has been applied to the calculation of advance ratio, is presented in figure 7 as the ratio of free-air velocity to the tunnel-datum velocity (tunnel empty) as a function of the thrust disk-loading coefficient. The tunnel-wall correction was found to be dependent only on the thrust disk-loading coefficient for the range of tunnel speed and propeller operation used in these investigations.

The results presented in figure 7 show that, for the zero thrust condition, a correction of 2 percent is required to the tunnel-datum velocity. This correction is due to constriction of flow produced by the model alone in the presence of the tunnel wall. The velocity correction required because the propeller is operating in the presence of the tunnel wall is zero for the above condition. Consequently, the changes in the velocity correction shown in figure 7 are due entirely to propeller operation in the presence of the tunnel wall.

The tunnel-datum Mach number has not been corrected for tunnel-wall constraint. It can be shown that for the

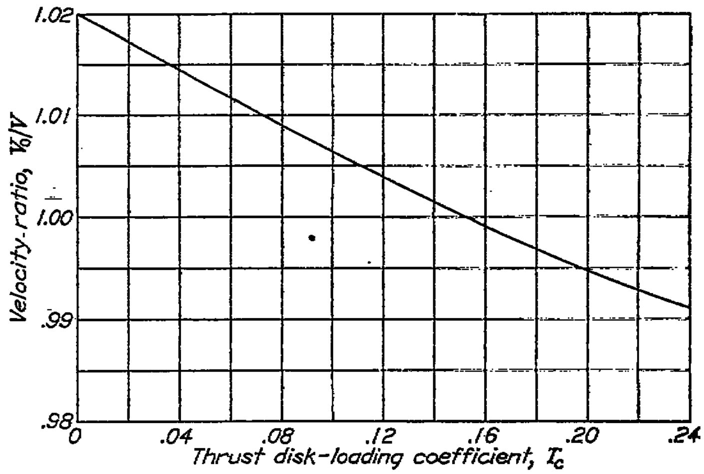


FIGURE 7.—Tunnel-wall interference correction.

range of velocity ratio shown in figure 7 the factor required to correct the tunnel-datum velocity or Mach number to free-stream condition is essentially the same as the velocity-correction factor.

**Buoyancy correction to thrust.**—Owing to the contraction of the propeller slipstream in the presence of the tunnel wall, the air outside of the slipstream undergoes an increase in static pressure with distance downstream from the propeller. This increase in static pressure gives rise to a buoyancy force on the model. The buoyancy force was evaluated from simultaneous measurements of the static pressure at orifices 6 inches apart in a circular tube extending to locations ahead of and behind the fuselage and installed approximately 6 inches from the wall of the tunnel. These measurements permitted evaluation of the buoyancy force from changes in the longitudinal pressure gradient (produced by changes in propeller thrust) in which the model was located. It was found that the buoyancy force was approximately 2 percent of the propulsive thrust for all operating conditions of the tunnel and propellers. This correction has been applied to the thrust results presented herein.

## RESULTS AND DISCUSSION

The basic characteristics for the NACA 4-(3)(08)-03 and 4-(3)(08)-045 two-blade propellers are presented in figures 8 and 9, respectively. For each value of the tunnel-datum Mach number, the propeller thrust coefficient, power coefficient, and efficiency are plotted against advance ratio. The variation of tip Mach number with advance ratio is also included. As used in this report, the tunnel-datum Mach number $M$ is not corrected for the effects of tunnel-wall constraint. The free-stream Mach number can be obtained by applying the tunnel-wall corrections presented in figure 7 to the tunnel-datum Mach number. Similarly, the corrected tip Mach number can also be obtained.

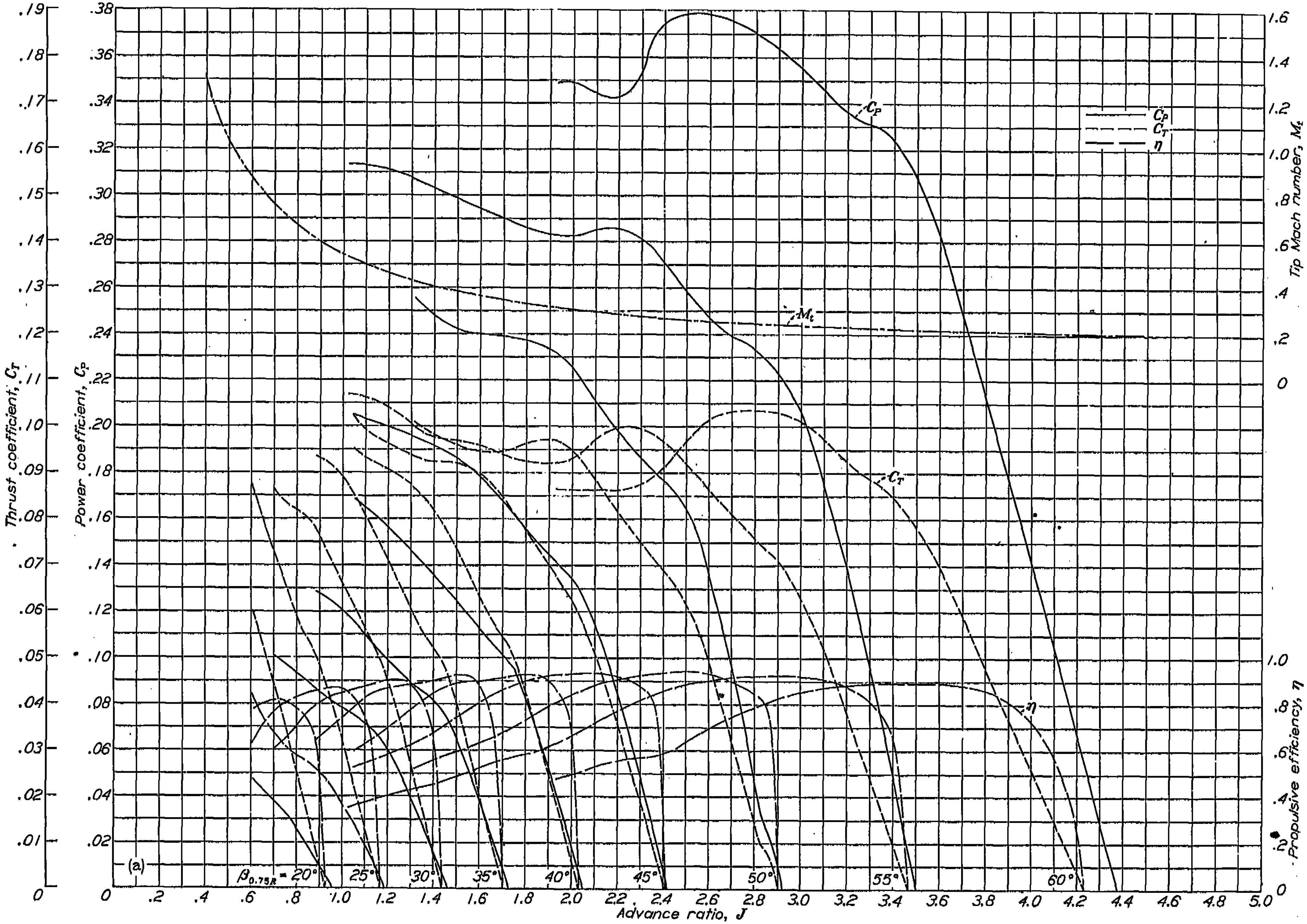


(a) $M=0.165$.

FIGURE 8.—Characteristics for the NACA 4-(3)(08)-03 propeller.

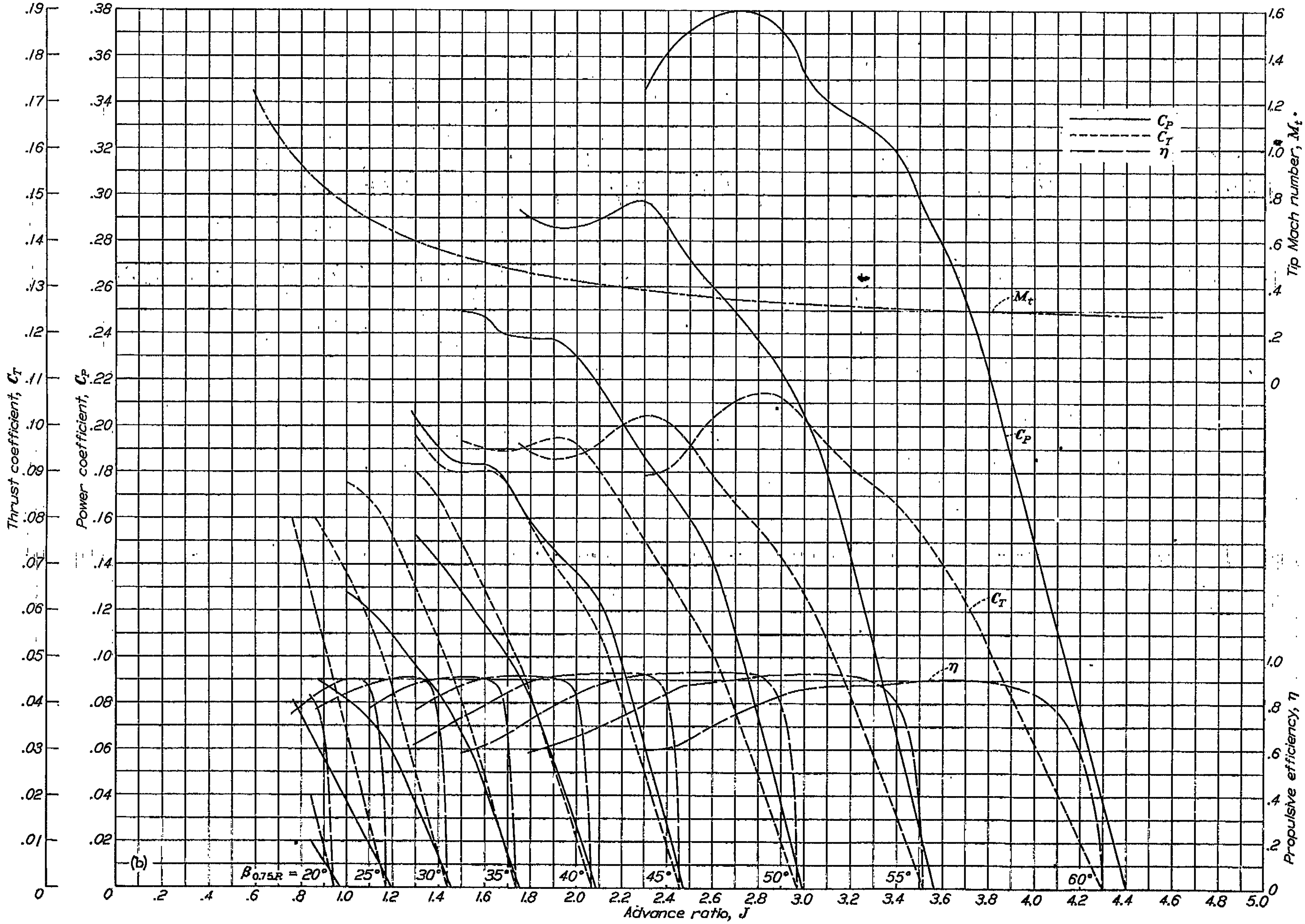


(b) $M=0.23$.

FIGURE 8.—Continued.

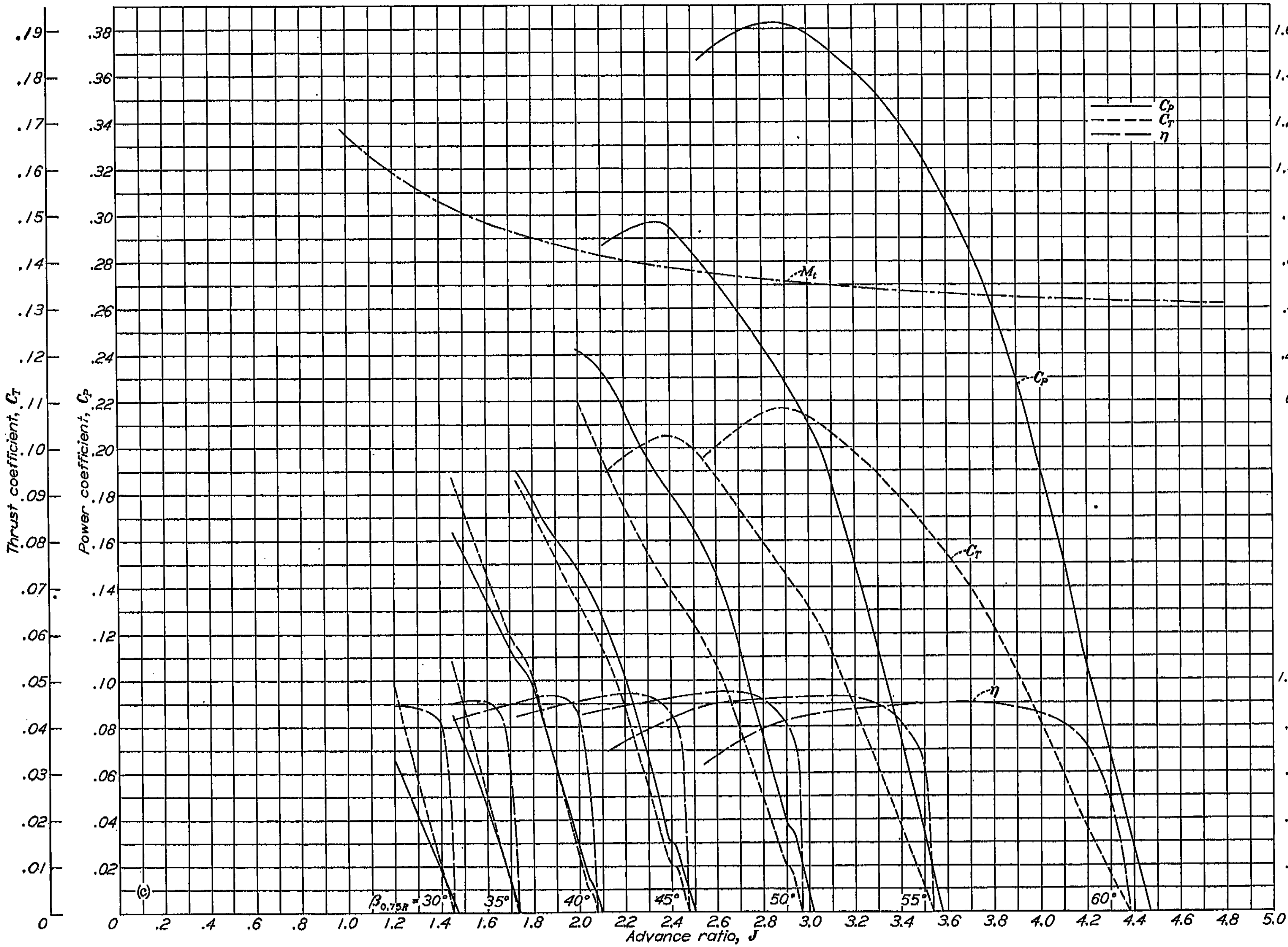


(c) $M=0.85$.

FIGURE 8.—Continued.

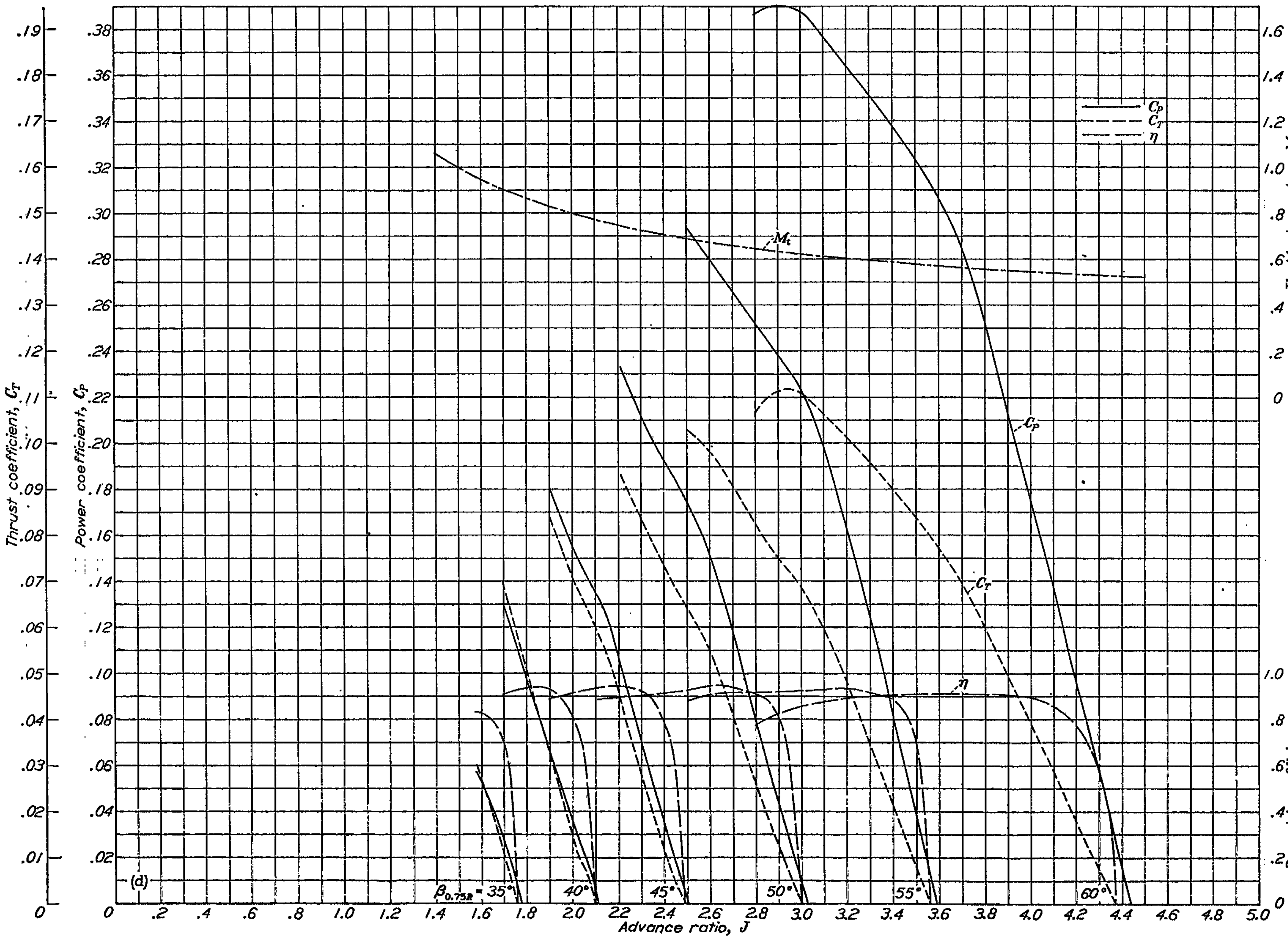


(d) $M$=0.48.

FIGURE 8.—Continued.

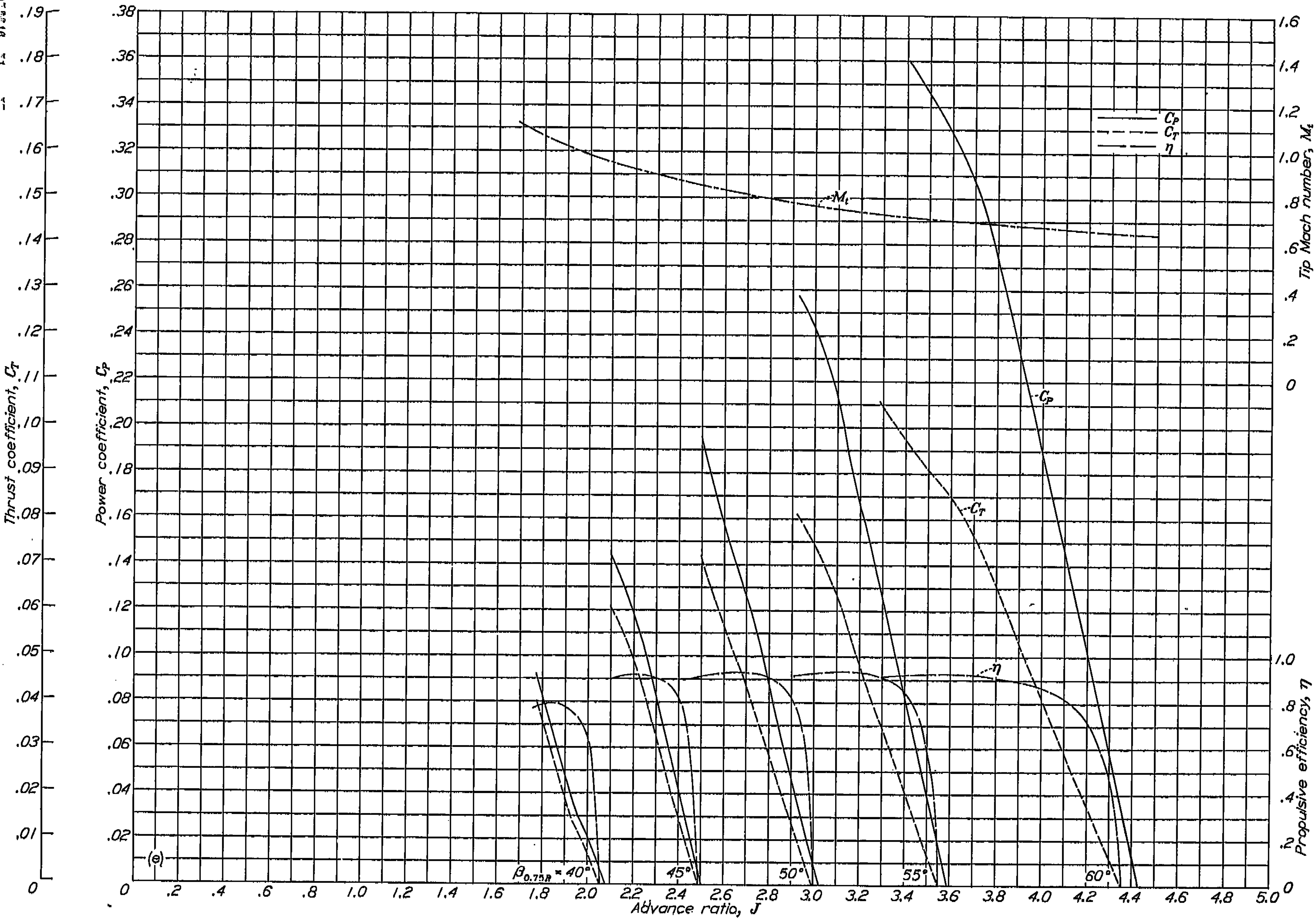


(e) $M$=0.53.

FIGURE 8.—Continued.

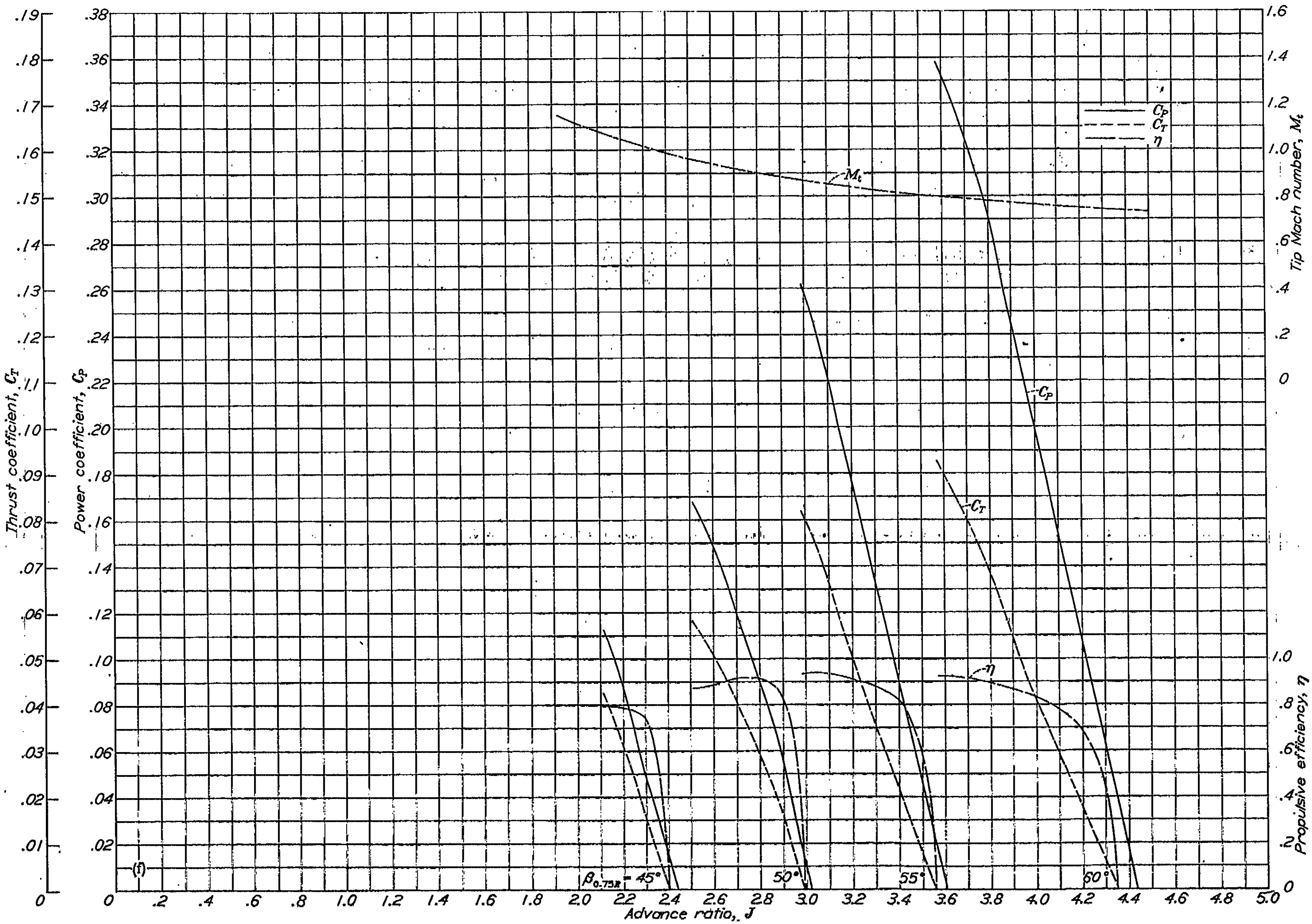


(f) $M=0.60$.

FIGURE 8.—Continued.

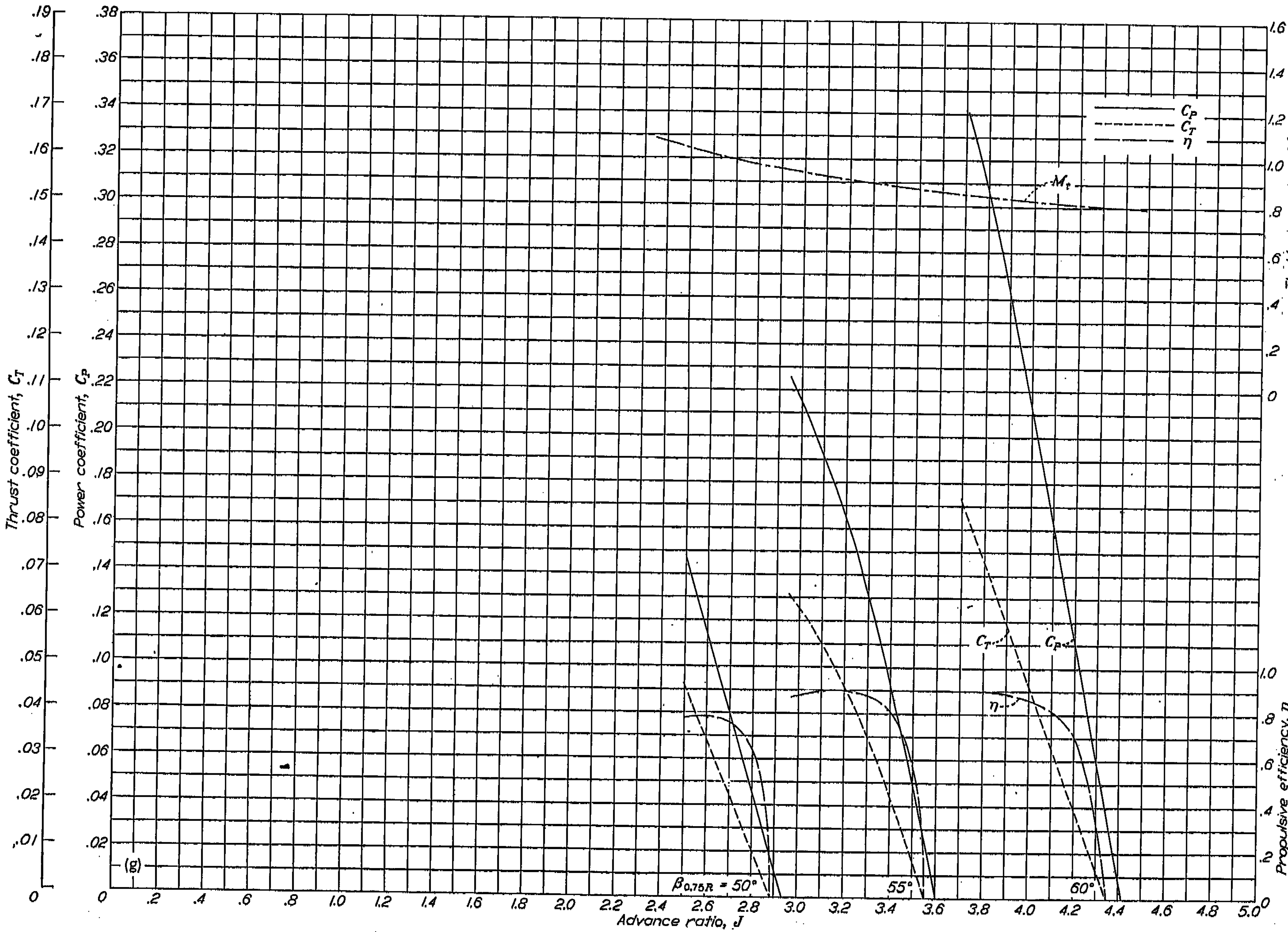


(g) $M$=0.65.

FIGURE 8.—Continued.

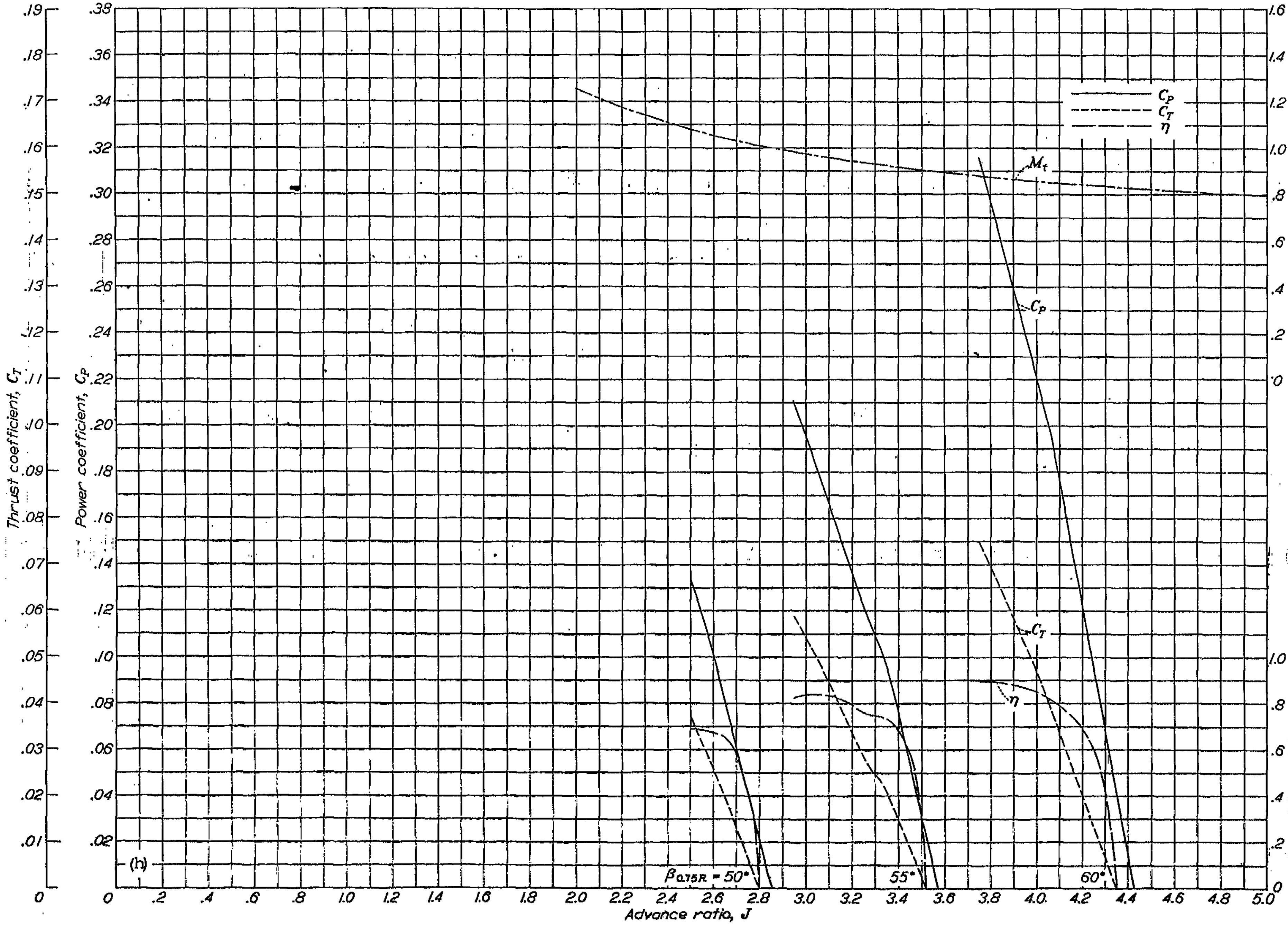


(h) $M$=0.675.

FIGURE 8.—Continued.

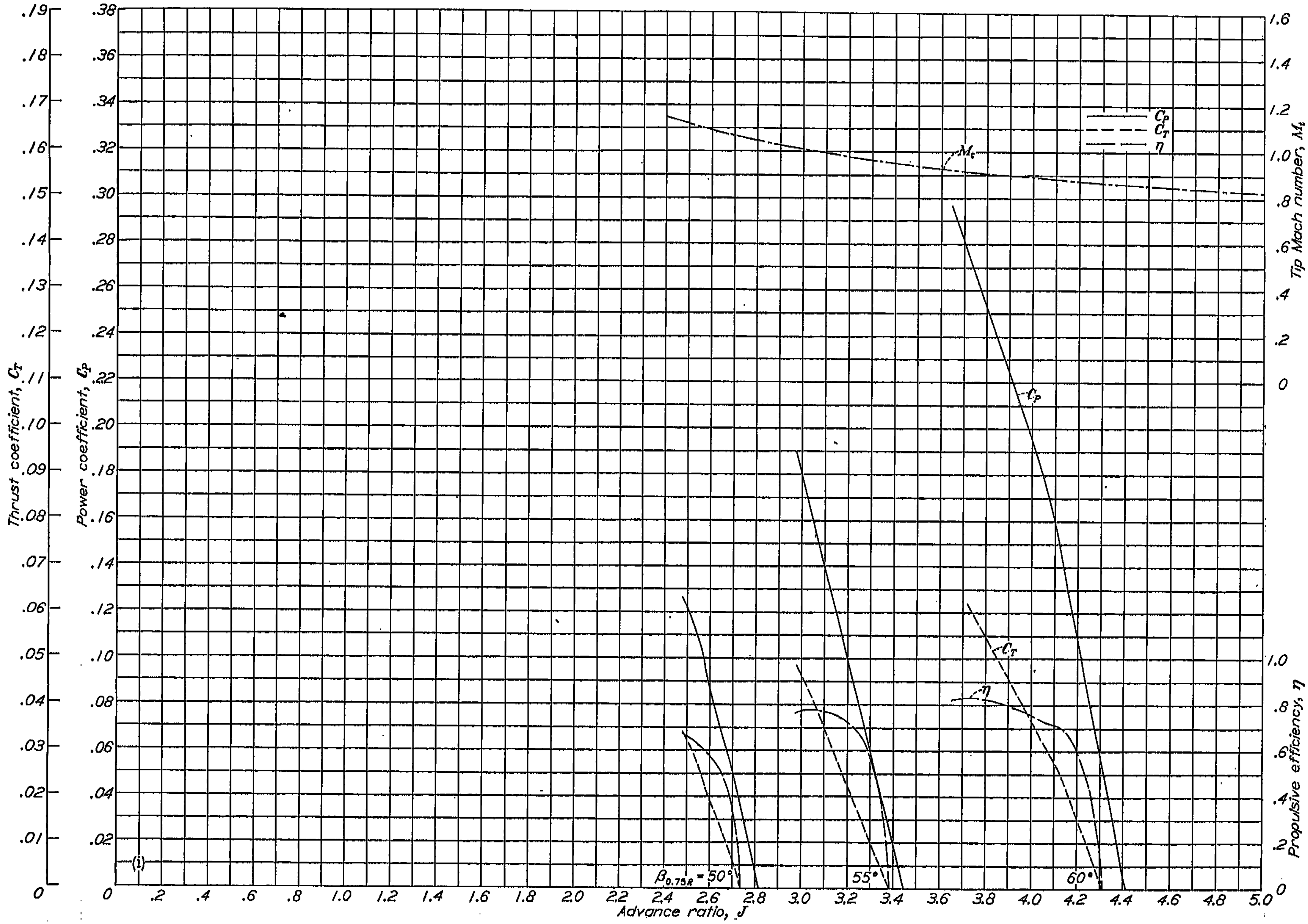


(i) $M=0.70$.

FIGURE 8.—Continued.

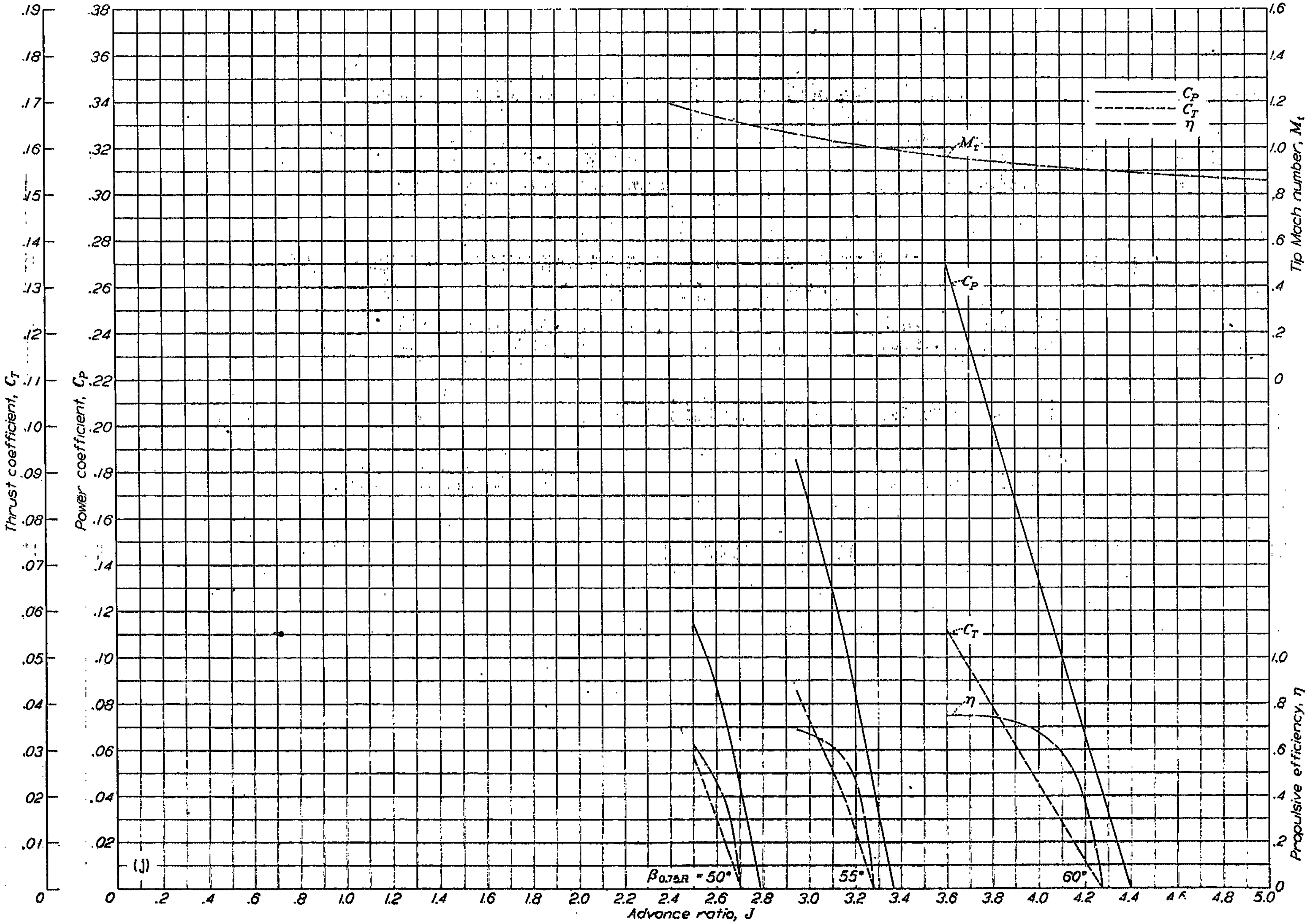


(j) $M=0.725$.

FIGURE 3.—Concluded.

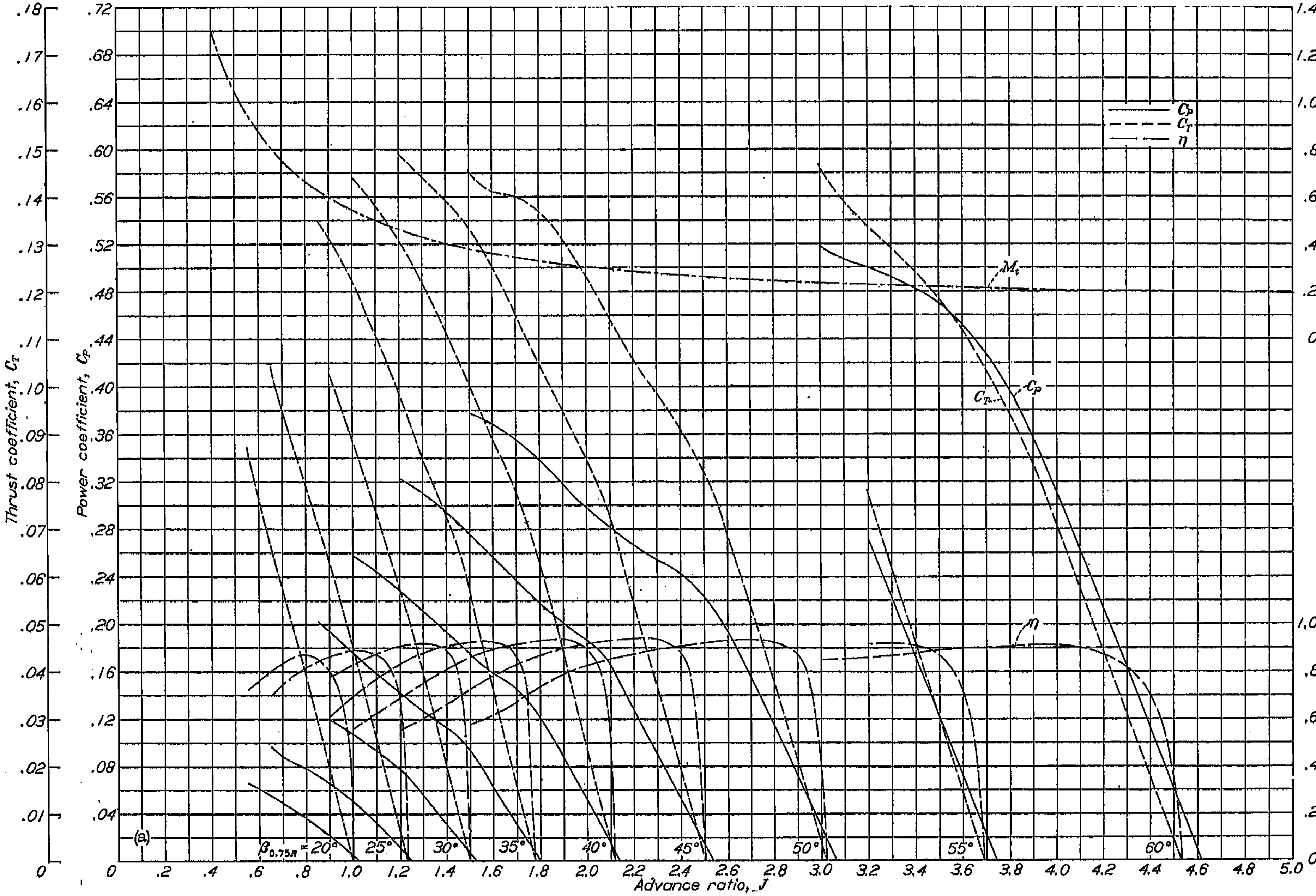


(a) $M$=0.165.

FIGURE 9.—Characteristics for the NACA 4-(3)(08)-045 propeller.

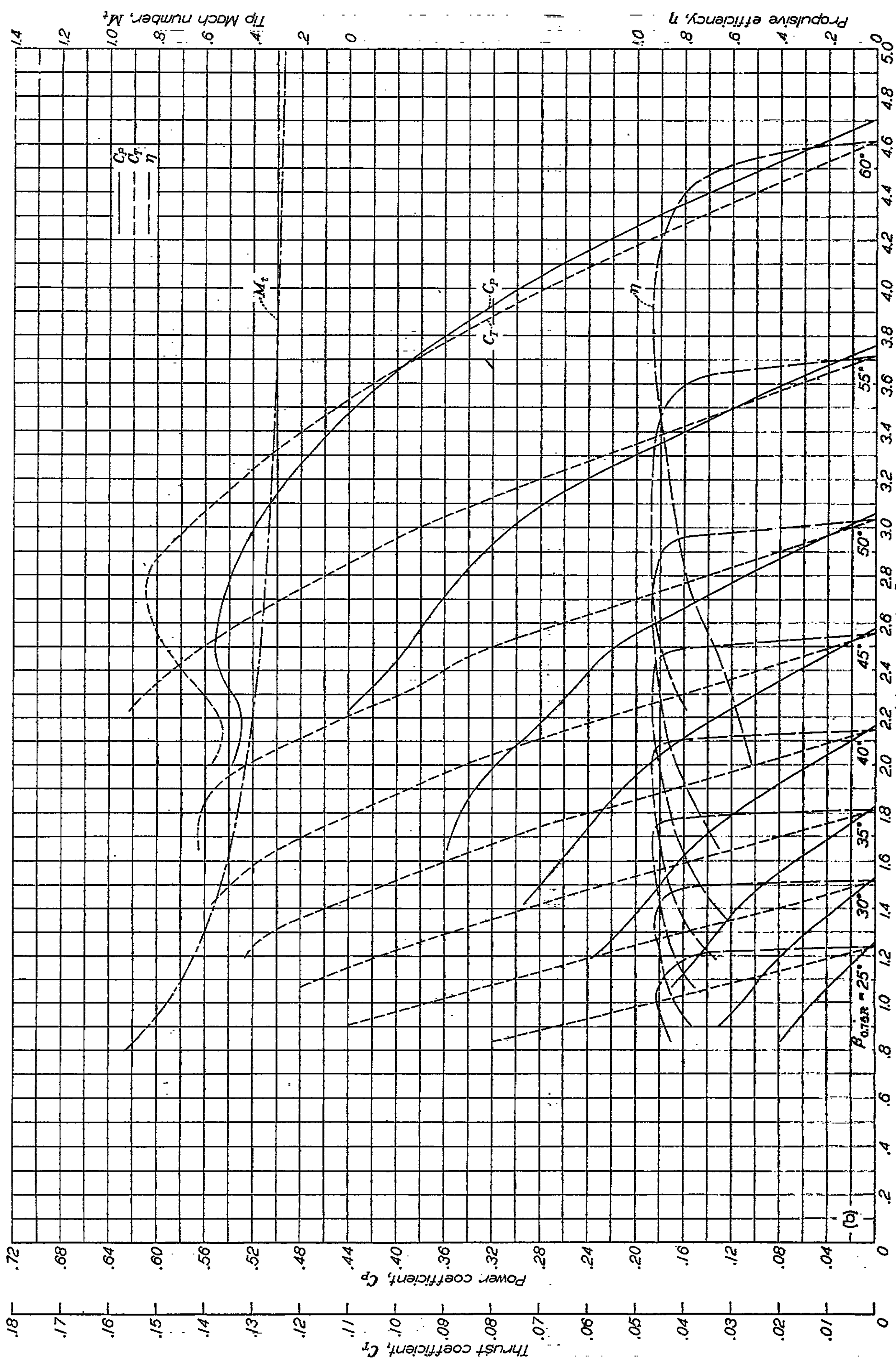


(b) $M=0.23$.

FIGURE 9.—Continued.

956646—51——58

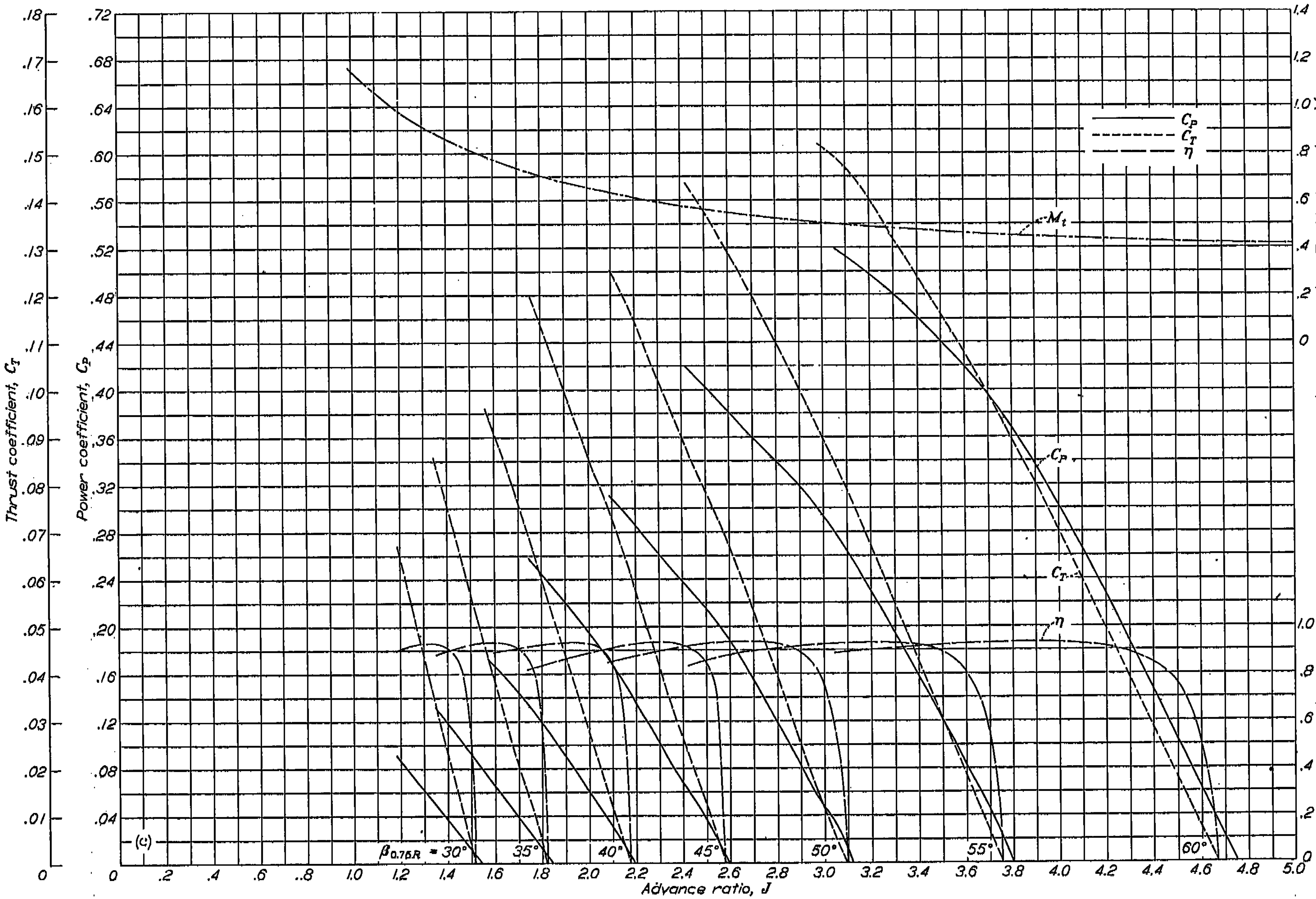


(c) $M$=0.85.

FIGURE 9.—Continued.

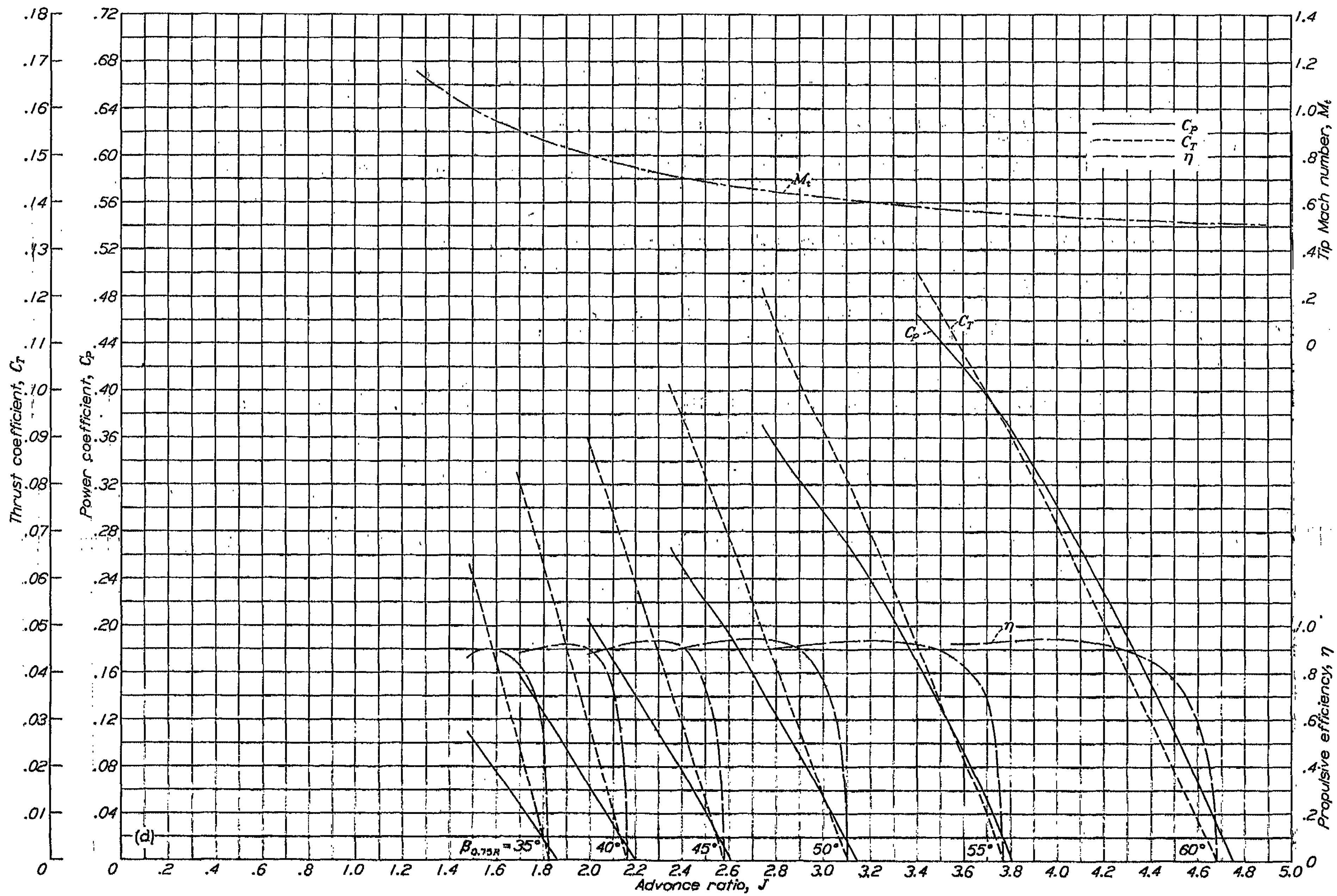


(d) $M$=0.43.

FIGURE 9.—Continued.

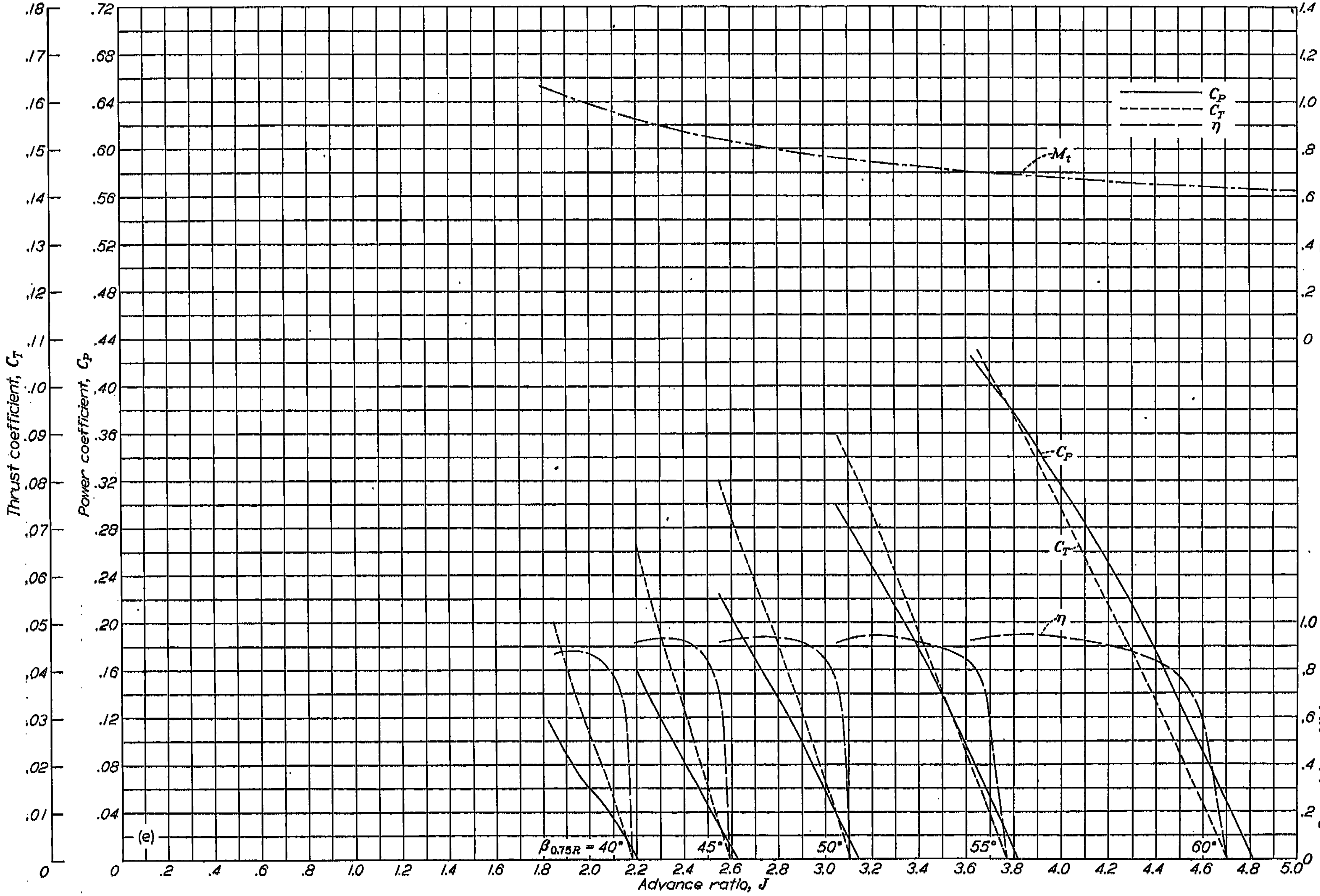


(e) $M=0.53$.

FIGURE 9.—Continued.

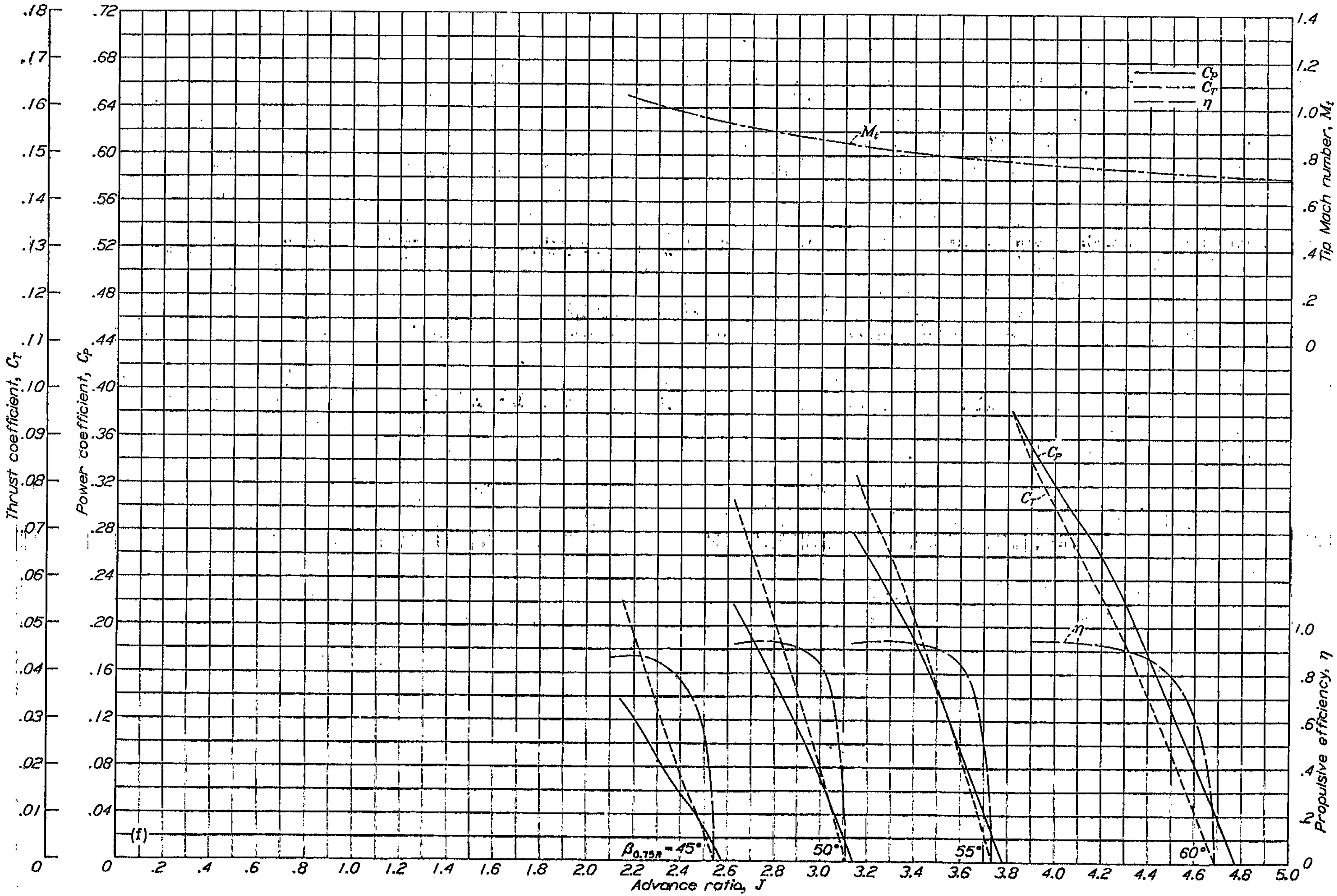


(f) $M=0.60$.

FIGURE 9.—Continued.

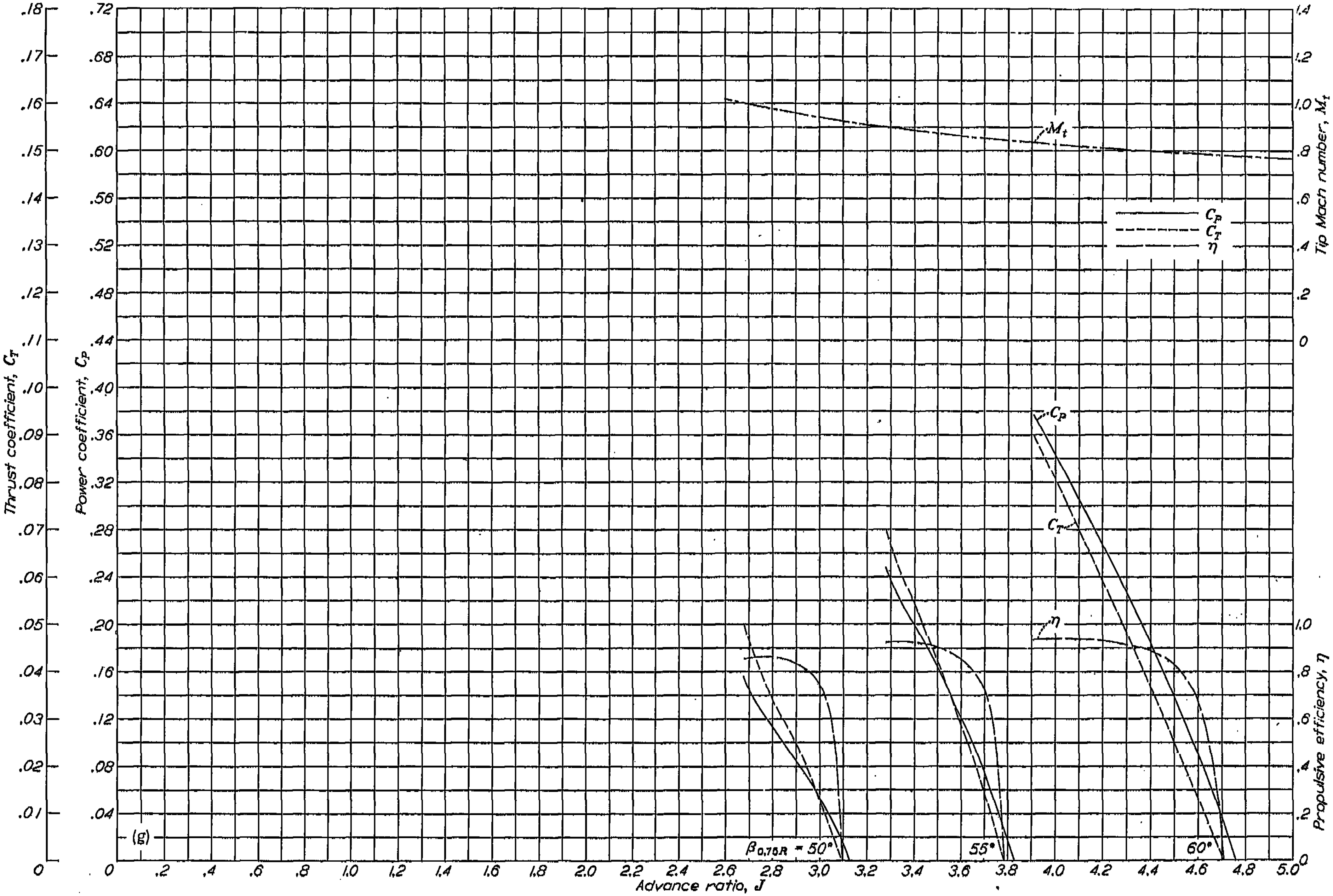


(g) $M=0.65$.

FIGURE 9.—Continued.

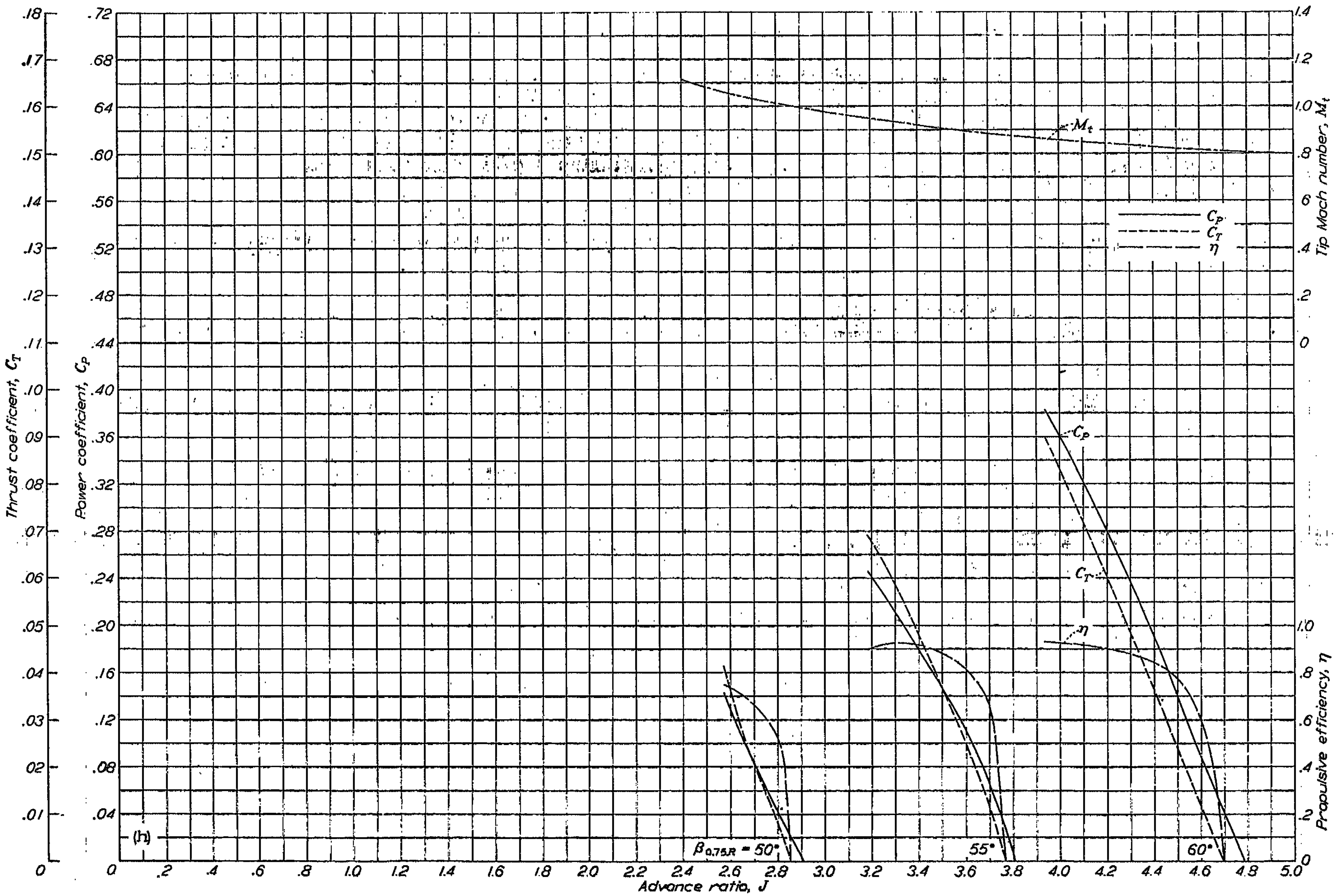


(h) $M=0.675$.
FIGURE 9.—Continued.

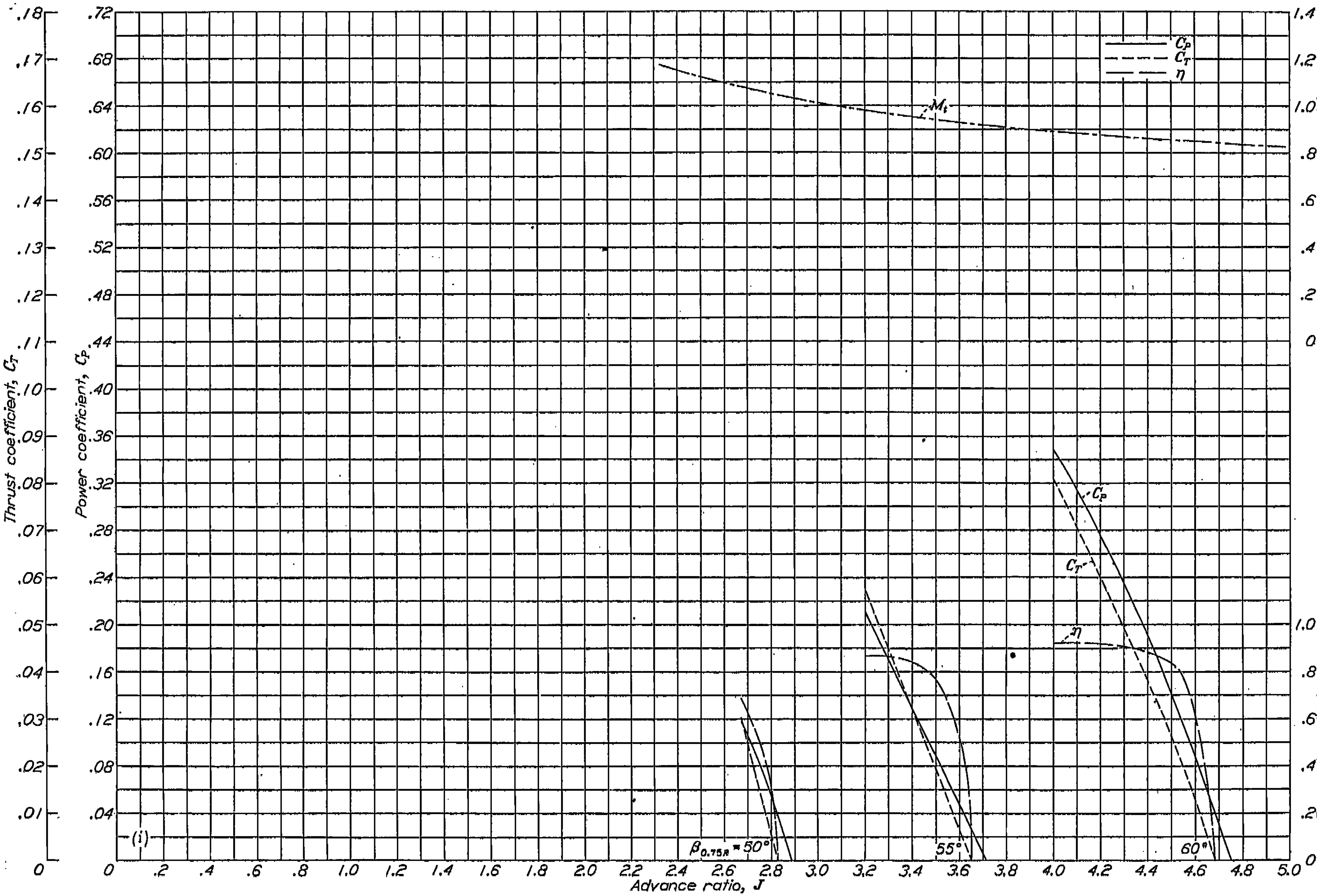


(i) $M$=0.70.

FIGURE 9.—Concluded.

## COMPRESSIBILITY EFFECTS

The general effects of compressibility on propeller performance shown by the results of the NACA 4-(3)(08)-03 and 4-(3)(08)-045 propellers are similar. Consequently, these effects will be illustrated by the results for the NACA 4-(3)(08)-03 propeller.

**Critical tip Mach number.**—The primary consideration in the operation of propellers at high forward speeds is the tip Mach numbers that can be reached before serious losses in maximum efficiency are encountered. These values are indicated by figure 10, which shows the variation of relative efficiency with tip Mach number for several blade angles. The relative efficiency $\eta_{max}/\eta_i$ is the ratio of the maximum efficiency at the tip Mach number being considered to the maximum efficiency at low speeds (at a tip Mach number of approximately 0.25). Propeller critical tip Mach numbers of the order of 0.88 to 0.91, depending upon the blade angle, are shown (correction of the tunnel-datum Mach number by use of the factors given in figure 7 results in corrected tip Mach numbers of 0.90 to 0.93). The highest value was obtained for a blade angle of 45°. At this blade angle, the propeller tested operates with its blade sections at practically their design or optimum lift coefficients; hence, it is for this condition of operation that the blade sections have their highest critical Mach number. Operation at blade angles other than 45° requires that the blade sections operate at lift coefficients other than the optimum values and hence lower critical Mach numbers can be expected. The variation of critical tip Mach number with blade angle is shown in figure 11. It can be expected that critical tip Mach numbers as high as those obtained for the blade angle of 45° can be obtained for the same loading at other blade angles, provided that the pitch distribution and solidity are modified to permit operation of the blade sections at their design lift coefficients.

**Envelope efficiency.**—The influence of compressibility on propeller performance is further illustrated in figure 12 by comparison of the envelope efficiencies obtained at various forward Mach numbers. Curves of approximately constant tip Mach number are also shown in the same figure. Serious losses in efficiency appear first at low values of advance ratio for any given forward Mach number. Such losses can be obtained with incorrect choice of diameter or gear ratio. Compromise designs involving increased diameter favoring climb or take-off may lead to important compressibility losses at high speed. The rapid decrease in efficiency with decrease of advance ratio and increase of forward Mach number emphasizes the importance of operation at proper values of advance ratio when the forward Mach number is high. Thus, one method for delaying compressibility losses to higher forward speeds is to reduce the tip Mach number by operating at high values of advance ratio.

**Efficiency loss at supercritical speeds.**—The efficiency loss at supercritical tip Mach numbers is linear within the speed range investigated and varies from approximately 9 percent to 22 percent per 0.1 increase in tip Mach number. (See fig. 10.) As with the critical tip Mach number, the rate of efficiency loss is dependent upon the blade angle and is a minimum at the design blade angle. Operation at blade angles other than the design value, which is approximately 45° for this propeller, leads to higher efficiency losses because the blade sections are operating at lift coefficients other than the design values. Lower critical speeds and larger drag losses consequently would occur. Furthermore, a greater proportion of the blade operates at higher section speeds at the higher blade angles if the tip Mach number is held constant. The magnitude of the efficiency losses at supercritical tip Mach numbers is sufficiently great to require

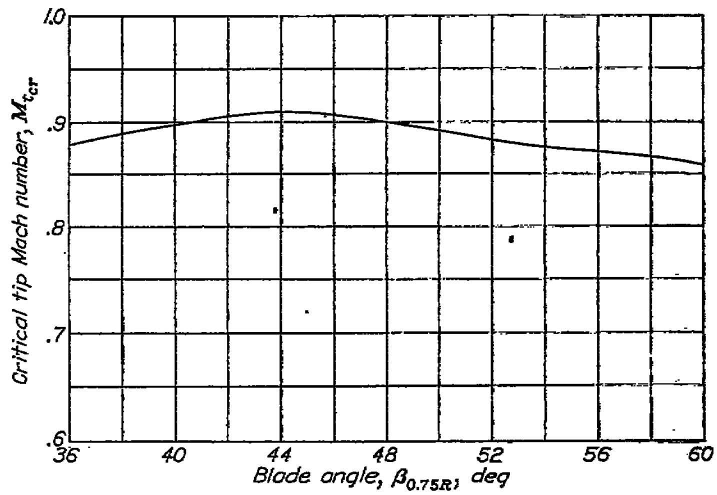


FIGURE 11.—Effect of blade angle on critical tip Mach number for NACA 4-(3)(08)-03 propeller.

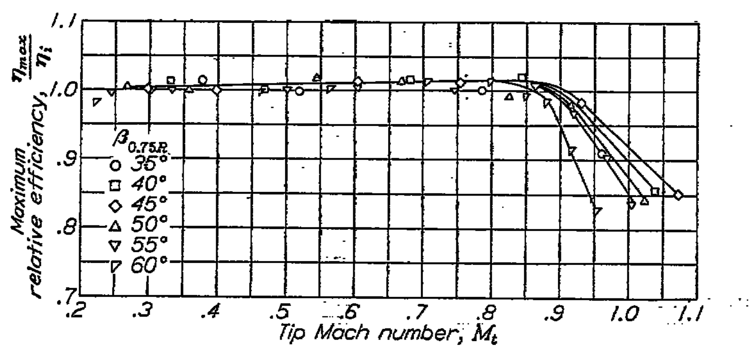


FIGURE 10.—Effect of compressibility on relative maximum efficiency for NACA 4-(3)(08)-03 propeller.

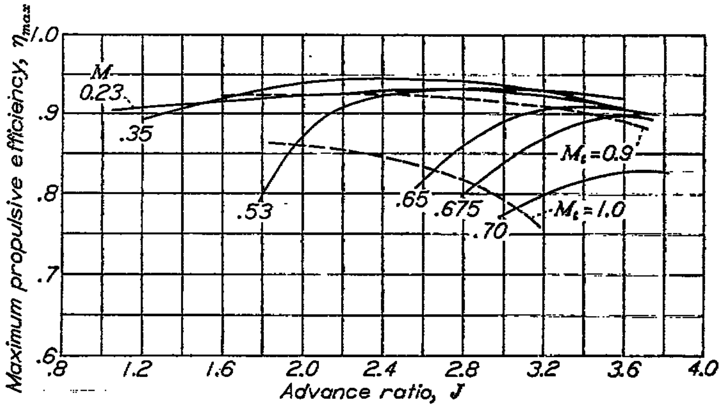


FIGURE 12.—Effect of compressibility on envelope efficiency for NACA 4-(3)(08)-03 propeller.

that such operation be avoided. In designs for which it may be impossible to avoid operating at supercritical tip Mach numbers, the variation of efficiency with blade angle emphasizes the need for selection of the proper pitch distribution.

The losses in efficiency due to compressibility effects are higher than those indicated by some previous research. High tip speeds generally are encountered with high-speed aircraft and hence at high values of the advance ratio and blade angle. Most previous investigations have been made at low forward speeds and low blade angles, and losses based on previous data therefore are an extrapolation when applied to determine performance at high values of advance ratio and blade angle. The most widely used method for application of high-tip-speed data over wide ranges in blade angle is given in references 6 and 7. This method consists in substituting the efficiency determined by tests at one blade angle in the expression for the efficiency derived from the simple blade-element theory and evaluating an effective drag-lift ratio of the blade. This drag-lift ratio is then substituted back in the same formula and applied to all values of advance ratio. The results obtained from this method of extrapolation as applied to propeller problems for high-speed airplanes can be expected to be optimistic, particularly for values of the losses above the propeller critical tip Mach number. This is true because the effective drag-lift ratio determined for the blades had been found from tests at low forward speeds and low blade angles for which the proportion of the blade above the section critical Mach number is smaller than that in normal operation at high speeds and high blade angles. A comparison of the efficiencies as calculated by the method of references 6 and 7 and the values obtained in the present investigation are shown in figure 13 (the tip Mach numbers have been corrected for tunnel-wall constraint). The critical tip Mach numbers are shown to be slightly lower and the losses, considerably greater than the extension or extrapolation of previously existing data indicates. Figures 10 and 13 also show slightly favorable effects of compressibility at subcritical Mach numbers, which have not been shown by previous information.

**Thrust and power coefficients.**—Studies of the compressibility effects based on efficiency alone are, of course, of primary importance in relation to airplane performance; they, however, are not completely illustrative of the types of change occurring because the efficiency is dependent upon the thrust and power coefficients and upon the advance ratio. It is conceivable that considerable variation in thrust and power coefficients at a given value of the advance ratio and blade angle can occur without affecting the efficiency to any great degree. The variations of thrust coefficient and power coefficient with forward Mach number at constant values of advance ratio for a blade angle of 45° are shown in figures 14 and 15, respectively. Such plots are equivalent in a sense to plots of airfoil lift coefficient against Mach number for constant angles of attack. Marked changes in the thrust and power coefficients occur and these changes are, in general, similar to the variation of airfoil lift coefficient with Mach number except at the lowest speeds at which the thrust and power coefficients appear to vary somewhat irregularly. This irregular variation (to be explained subsequently) is probably due to a change in advance ratio for zero thrust and power. If profile drag

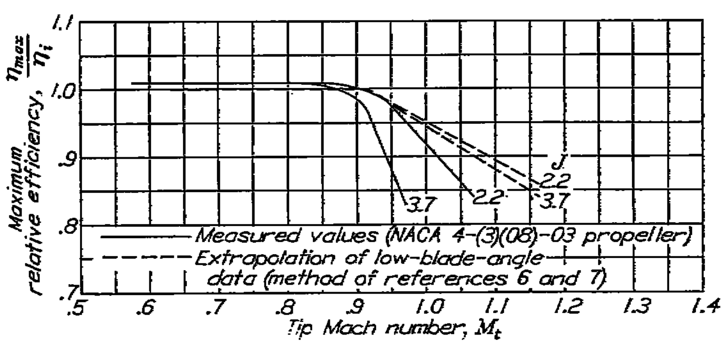


FIGURE 13.—Comparison of relative maximum efficiencies with values obtained by a conventional method of extrapolation.

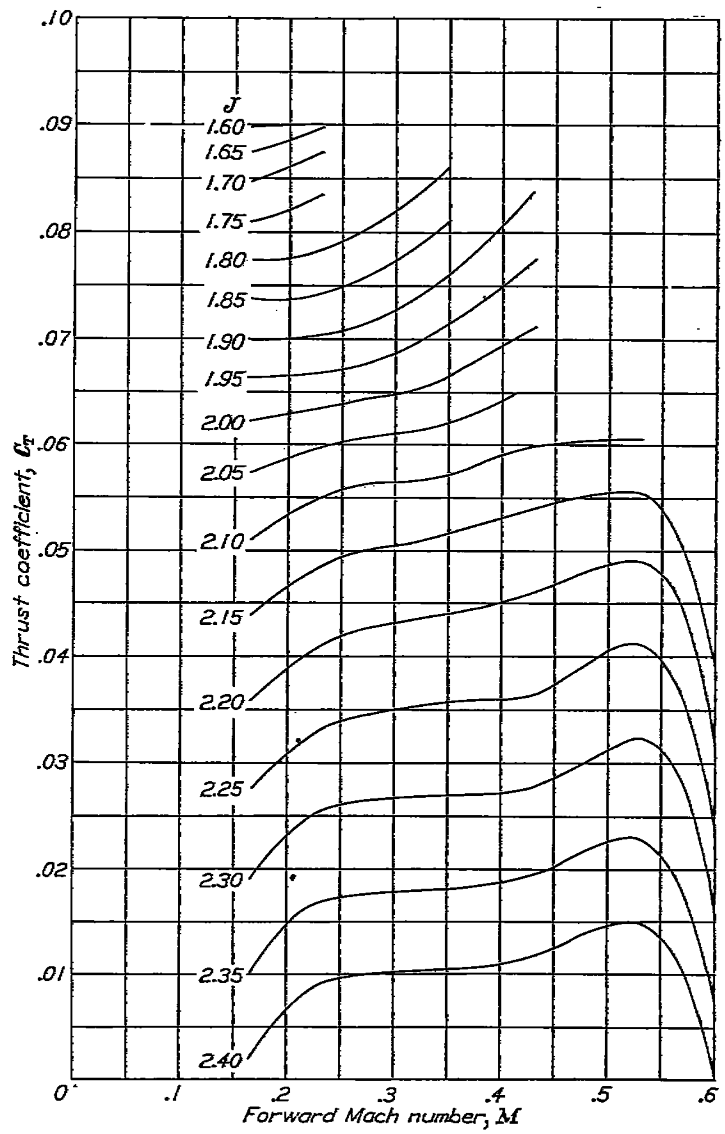


FIGURE 14.—Variation of thrust coefficient with Mach number for constant values of advance ratio for the NACA 4-(3)(08)-03 propeller. $\beta_{0.75R}$, 45°.

is neglected, the thrust and power coefficients for constant advance ratio and blade angle could be expected to vary with Mach number as airfoil lift coefficient varies with Mach number for a fixed angle of attack. Theoretically, for an airfoil, this variation in lift coefficient is proportional to $\frac{1}{\sqrt{1-M^2}}$ and, for the propeller with the thrust and power both having a similar variation, no effect on the efficiency is found. The effect of compressibility on efficiency in the subcritical range (fig. 10) is favorable; hence, it is indicated that some increase in blade-section lift-drag ratio must occur as the speed is increased up to the critical value. As basic airfoil data have also shown a slight increase in lift-drag ratio with increase in speed or Reynolds number, particularly at low values of the Reynolds number, the small effect on propeller efficiency shown by figure 10 is to be expected.

The variation in the advance ratio for zero thrust and power coefficients at low speeds is not readily understood. Drag variation alone cannot account for the effect because drag-curve variation would tend to have the opposite effects on thrust-coefficient and power-coefficient values. Variation of the angle of zero lift of the blade sections is indicated. The effect of compressibility on thrust coefficient is shown in figure 16. It will be noted, however, that the variation in advance ratio for zero thrust and zero power which occurs at low speeds tends to disappear as the speed of the air stream is increased. The variation may be due to some Reynolds number effect. The shape of the curves indicates that a constant value of the zero-thrust and zero-power advance ratio is reached at Reynolds numbers and Mach numbers below the critical tip speeds; hence, the Reynolds number of the tests is probably sufficiently large to permit direct application to most full-scale problems.

At the highest Mach numbers investigated, marked decreases occur in thrust coefficient, power coefficient, and

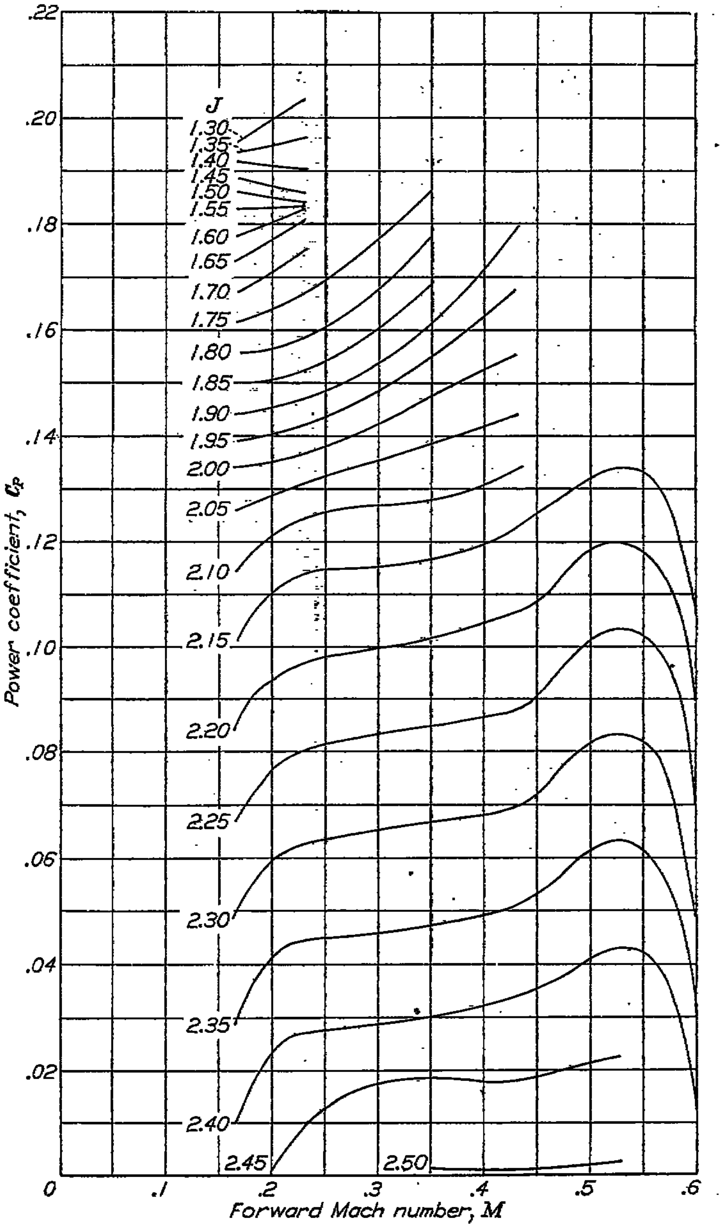


FIGURE 15.—Variation of power coefficient with Mach number for constant values of advance ratio for the NACA 4-(3)(08)-03 propeller. $\beta_{0.75R}$ 45°.

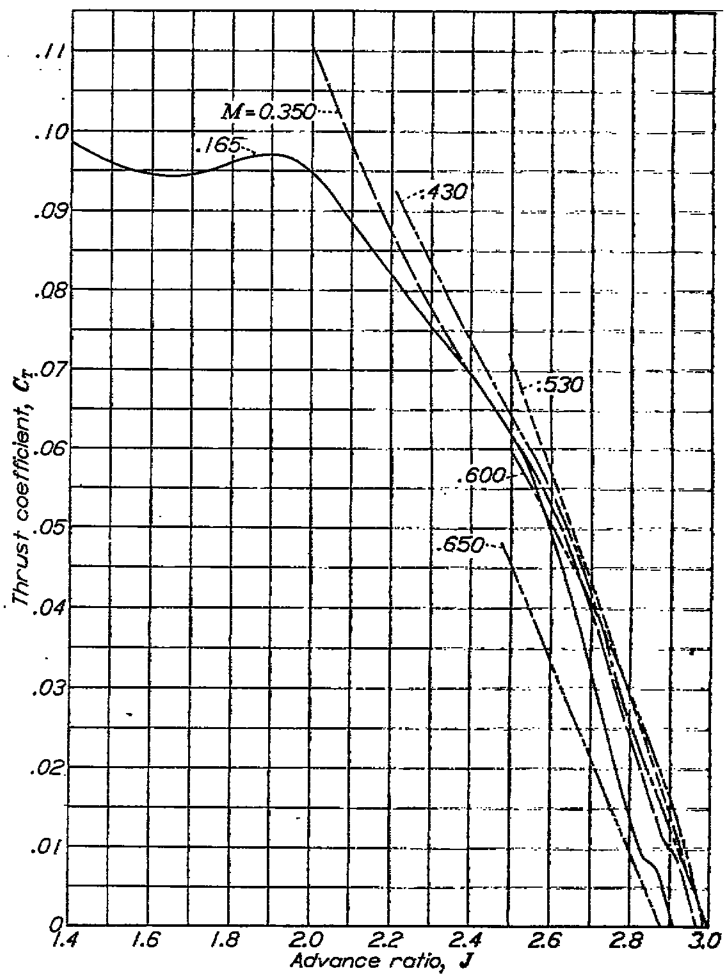


FIGURE 16.—Effects of compressibility on thrust coefficient for the NACA 4-(3)(08)-03 propeller. $\beta_{0.75R}$, 50°.

advance ratio for zero values of the thrust and power. These changes are entirely in accordance with previous airfoil data which have shown large decreases in lift coefficient, increases in drag coefficient, and change in angle of zero lift. The similarity of the compressibility effects observed to those found for airfoils is further illustrated in figure 16. At the low speeds, some irregularities in the thrust-coefficient curves appear and these irregularities are somewhat similar to those that have been found in lift curves at low Reynolds numbers. With increase of speed, the irregularities disappear. There is an apparent increase in the maximum lift coefficient with increase of speed that is evidenced by the higher thrust coefficients obtained for the high-speed data at the lower advance ratios. The slope of the thrust-coefficient curve increases with increase in speed in essentially the same way as the lift-curve slope increases with Mach number and, finally, there is a shift of the thrust curve to the left which corresponds to the shift in lift curve that has been found in tests of airfoils at high airspeeds.

### COMPRESSIBILITY AND SOLIDITY EFFECTS

The effects of compressibility and solidity on propeller performance presented in the following discussion are based on a comparison of results of the NACA 4–(3)(08)–03 and 4–(3)(08)–045 two-blade propellers, the basic characteristics of which are given in figures 8 and 9.

**Critical tip Mach number.**—The effect of solidity on the critical tip Mach number is indicated in figure 17 which shows the variation of the relative maximum efficiency with tip Mach number for several blade angles. Increasing the blade solidity has a favorable effect on critical speed, and, within the range of tip speed investigated, the losses attained with the wider blade are appreciably smaller than for the narrower blade. At the design blade angle (approx. 45°), the wider blade increased the critical tip Mach number by approximately 0.03. Smaller increases in critical tip Mach number occurred at other blade angles.

The favorable effect on critical tip speed produced by increased blade width is probably due principally to the lower lift coefficient of the wider blade at its maximum efficiency. The ratio of the thrust coefficients at maximum efficiency for the two blades at the design blade angle is shown in figure 18. Over the entire range of tip Mach number, the ratio of the thrust coefficients is appreciably less than the ratio of blade solidities. This ratio, however, is sensitive to the fairing of the efficiency curves near the peak of the curves; consequently, the values shown in figure 18 are to be considered in a qualitative sense only. At the highest Mach numbers, the maximum efficiencies of the two propellers occur at approximately the same value of thrust coefficient. The wider blade consequently reaches maximum efficiency at lower values of blade-section lift coefficient; hence, higher critical Mach numbers would be expected.

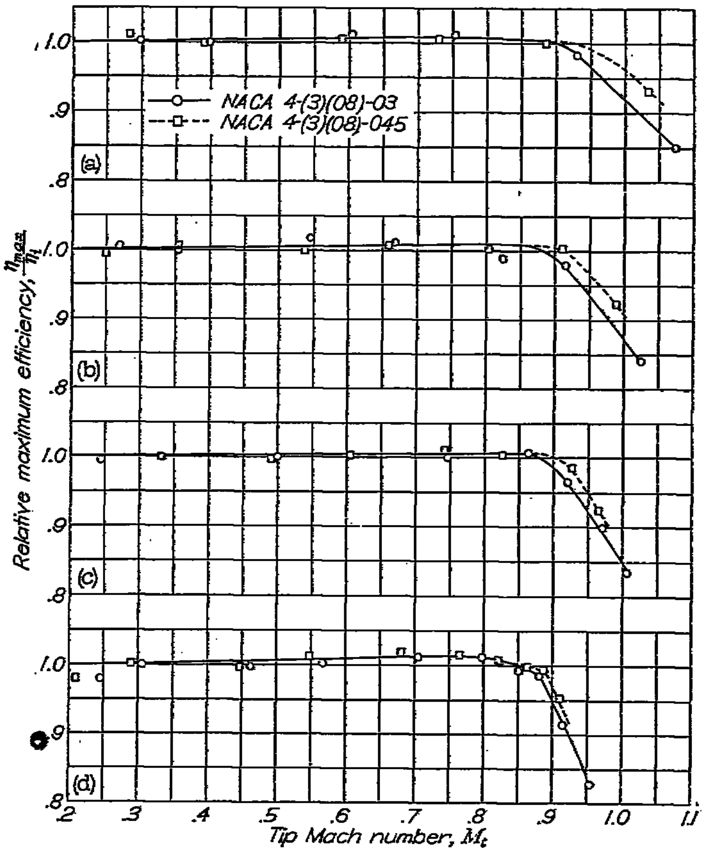


(a) $\beta_{0.75R}=45°$.
(b) $\beta_{0.75R}=50°$.
(c) $\beta_{0.75R}=55°$.
(d) $\beta_{0.75R}=60°$.

FIGURE 17.—Effect of compressibility and solidity on relative maximum efficiency.

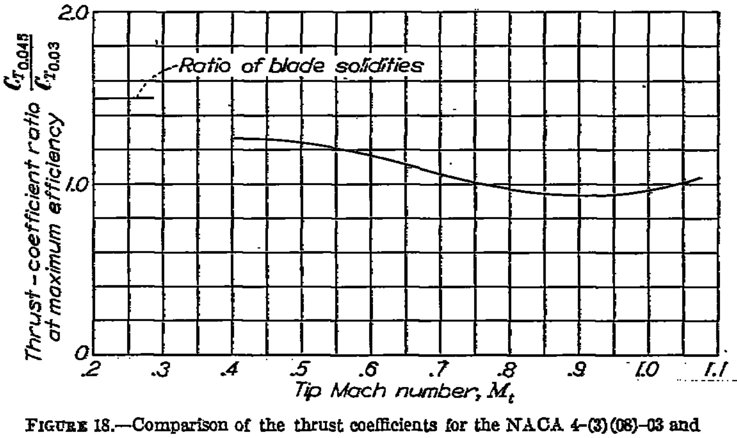


FIGURE 18.—Comparison of the thrust coefficients for the NACA 4-(3)(08)-03 and NACA 4-(3)(08)-045 propellers at maximum efficiency; $\beta_{0.75R}$, 45°.

**Envelope efficiency.**—Envelope efficiency curves for both propellers are presented in figure 19 for several values of forward Mach number. Lines corresponding to the tip Mach numbers of 0.9 and 1.0 are also shown. At the lowest forward Mach number $M$=0.23, the tip Mach numbers are less than the critical values shown in figure 17; therefore, no compressibility losses are encountered in the speed range shown. The envelope curves are flat and little difference occurs in efficiency for the two blade designs. With increase of forward speed, however, the tip Mach numbers exceed the critical values first, at the low advance ratios. Decreases in envelope efficiency occur that are greater than those for the narrower blade. Important decrements in envelope efficiency appear to start at a tip Mach number of approximately 0.9.

At high forward speeds, appreciably higher efficiencies are obtained with the wider blade. For a forward Mach number of 0.70, the envelope efficiency for the wider blade is from 7 to 10 percent higher than that for the narrower blade.

The values of efficiency obtained at high forward speeds are interesting. A forward Mach number of 0.70 corresponds to speeds of 463 to 532 miles per hour, depending on the altitude. These data indicate that efficiencies somewhat greater than 90 per cent can be obtained at these speeds provided that the advance ratio and solidity are maintained in specific ranges. As these particular propellers have higher blade-section thickness ratios at least over the outer portion of the blades than may be necessary, it appears probable that currently obtained low-speed efficiencies can be maintained to sea-level speeds of the order of 550 miles per hour. Applications of these data to high-speed-propeller problems are currently being studied.

**Power disk loading and maximum efficiency.**—Actual propeller efficiencies are determined by the induced loss and the blade section drag loss. In the ideal case, the induced efficiency is a function of the power disk-loading coefficient. In the practical application of propellers, the efficiencies obtained are less than the ideal efficiency by an amount that is determined by the blade-section characteristics and the disk-load distribution. The disk-load distribution for a propeller operating away from its design condition may have a large effect on efficiency. At maximum efficiency, however, the effects of load-distribution variations are relatively small and the differences between the ideal efficiency and the maximum efficiency at a given blade angle are due principally to the blade-section characteristics. Comparison of the maximum efficiency obtained in these tests with the ideal efficiency for several Mach numbers over the range of power loading investigated therefore illustrates the influence of the blade aerodynamic characteristics on the over-all propeller efficiency.

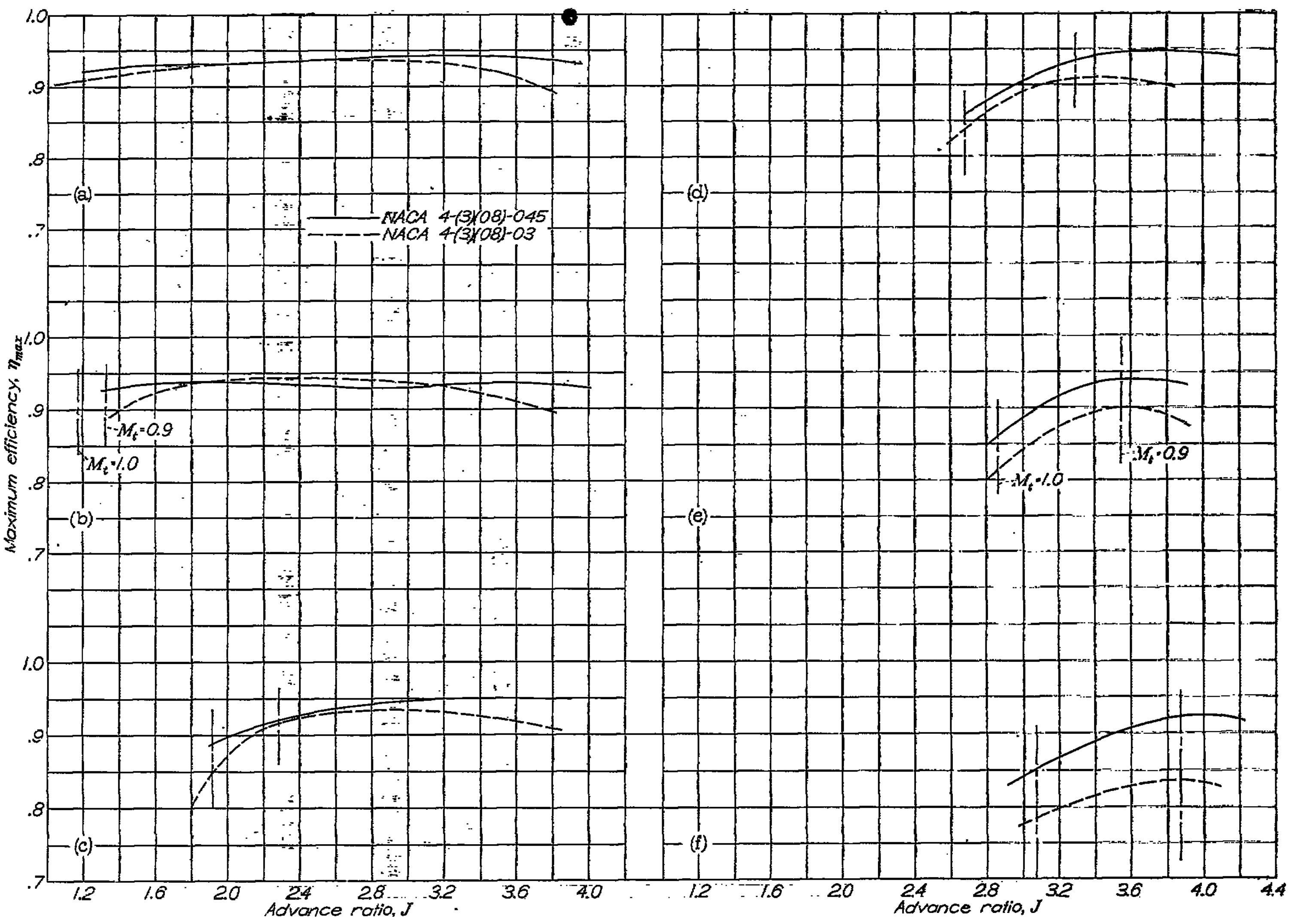


(a) $M$=0.23.
(b) $M$=0.35.
(c) $M$=0.53.
(d) $M$=0.65.
(e) $M$=0.675.
(f) $M$=0.70.

FIGURE 19.—Effects of compressibility and solidity on envelope efficiency.

Figure 20 shows the maximum efficiencies for both propellers, as determined from this investigation, plotted as functions of the power disk-loading coefficient $P_c$ for several values of forward Mach number. The ideal efficiency given by the axial-momentum theory is also shown in figure 20. At very low values of $P_c$, the measured propeller efficiencies show a sharp decrease because of the blade drag. Except for extremely low values of $P_c$, the general trend of measured efficiency should follow the theoretical trend. It is apparent also that the wider blade generally has higher efficiency, particularly as $P_c$ increases.

At low speeds, the difference between the ideal and actual efficiencies obtained is of the order of 5 to 8 percent, dependent upon the power loading. Over a part of the range, it is probable that a small part of this difference may be due to the existence of nonoptimum load distribution. The whole difference is small and the fact that a part of this difference could be due to blade-load distribution indicates that the propellers closely approximate optimum aerodynamic designs. Because the sections employed are the NACA 16 series, which have the highest critical speed of all propeller sections now available, the maximum efficiencies obtained over the entire speed range are probably close to the maximum now obtainable.

The variation in efficiency due to compressibility effects is shown by comparison of the data for the various Mach numbers. The predominant characteristic difference is the sharp decrease in efficiency with power loading that occurs at the higher speeds. The range of power disk-loading coefficient over which high efficiencies can be obtained decreases markedly at very high Mach numbers. As at low speeds and high power disk-loading coefficients, the wider blade shows the higher efficiency. The range, however, of power disk-loading coefficient covered is too small to permit a general conclusion. This phase of the problem is being investigated further.

From considerations of propeller design, probably the most significant conclusion indicated by the results presented in figure 20 is the large decrease in range of power loading for high efficiencies that occurs with increase of speed. For high-speed airplanes, the propeller design becomes much more critical. With high efficiency occurring only for a small range of power disk-loading coefficient, the choice of diameters, gear ratios, and solidities desired is

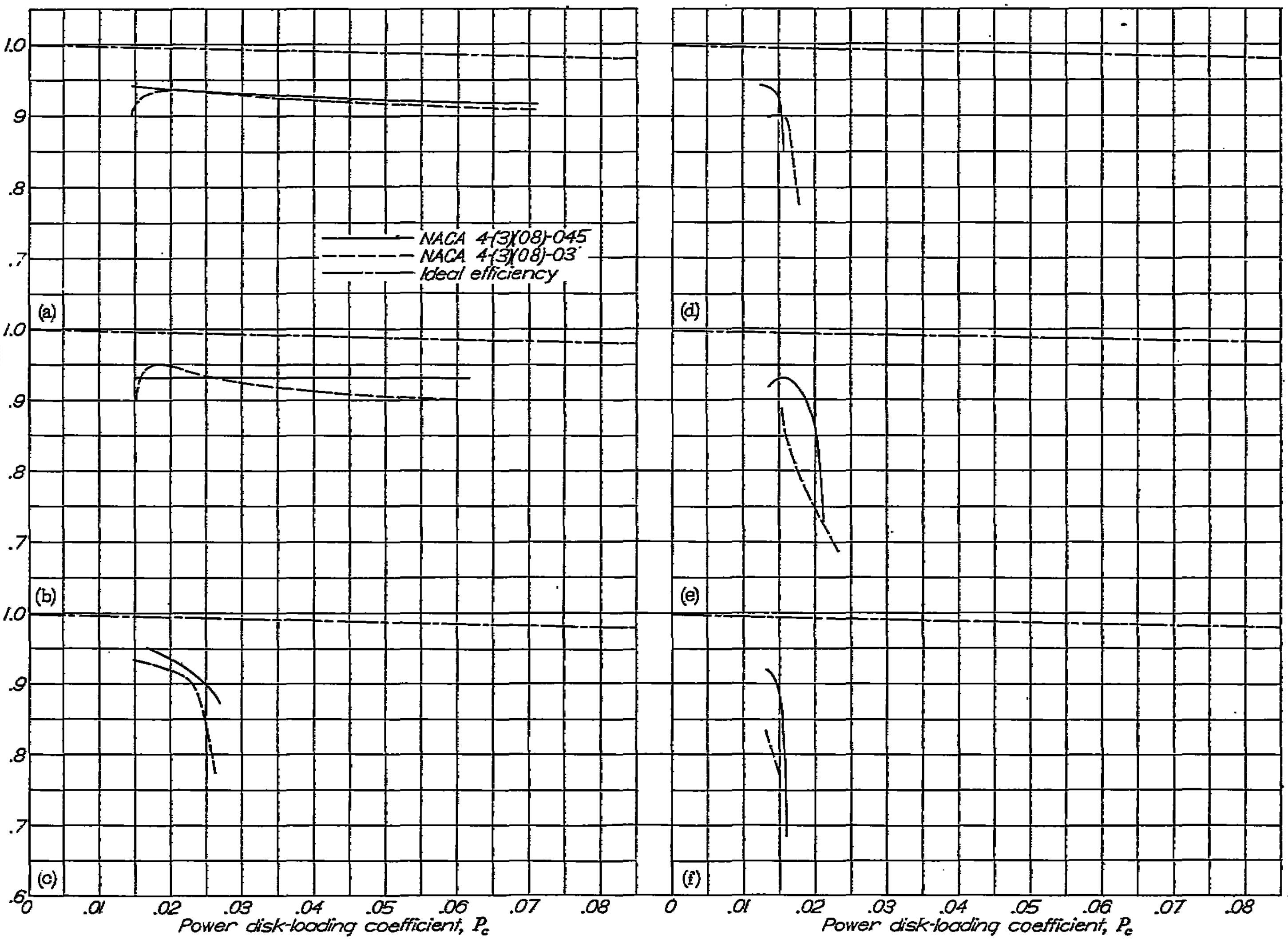


(a) $M$=0.23.
(b) $M$=0.35.
(c) $M$=0.53.
(d) $M$=0.65.
(e) $M$=0.675.
(f) $M$=0.70.

FIGURE 20.—Effect of power loading on maximum efficiency.

severely limited and it will likely prove necessary to design propellers for high-speed aircraft to suit particularly each individual application.

**Operation at constant power coefficient.**—As directly applied to aircraft, it is important to know the effects of design changes and speed increases in relation to the power coefficient. In many applications of operation at constant speed and hence at substantially constant power coefficient, large gains in climb efficiency may be obtained by increasing the propeller solidity. This effect is illustrated in figure 21 which shows the variation in efficiency with advance ratio for a constant value of power coefficient. At this value of power coefficient, low-speed data would thus indicate that the principal advantage of the wider blade occurs only at low values of advance ratio. In this respect, these results are in agreement with other low-speed test data. Under actual operating conditions, however, the higher advance ratios would be obtained at higher forward speeds. The results presented in figure 21 (b) rather than in figure 21 (a) are therefore applicable to operation at high advance ratio. These results show significantly higher efficiency for the wider blade. The chosen value of $C_P$=0.15 corresponds to maximum efficiency at a moderately high blade angle. The data presented in figure 21 (a) are for a forward Mach number in the climbing range and in figure 21 (b) for a forward Mach number in the high-speed range. At low advance ratio, which would be the operating condition at the lower speed (climb), higher efficiency is obtained with the wider blade. At this same forward speed but at high advance ratio, the efficiencies are the same for both propellers. The gains obtained through application of blades of increased solidity thus appear to exist over the entire normal operating range and the advantages possible through increased solidity are underestimated by the usual propeller data at low forward speed.

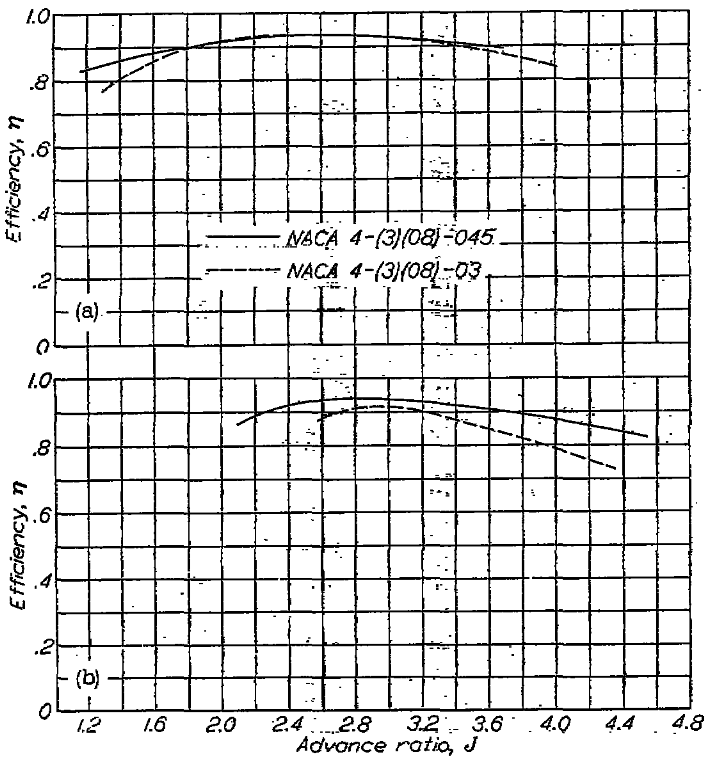


(a) $M$=0.23.
(b) $M$=0.60.

FIGURE 21.—Comparison of efficiency at constant power coefficient; $C_P$, 0.15.

## CONCLUSIONS

Results of investigation of two-blade propellers having NACA 4-(3)(08)-03 and NACA 4-(3)(08)-045 blade designs in the Langley 8-foot high-speed tunnel through a range of blade angle from 20° to 60° for forward Mach numbers from 0.165 to 0.725 show the following effects of compressibility and solidity on propeller performance:

1. Serious losses in propeller efficiency occurred at tip Mach numbers in excess of 0.91.
2. The effect of compressibility losses on maximum efficiency was dependent upon the blade angle and varied in magnitude from approximately 9 to 22 percent per 0.1 increase in tip Mach number above the critical value.
3. The range of peak efficiency, as shown by the envelope-efficiency curves, decreased markedly with increase of forward speed.
4. Compressibility losses could be delayed to successively higher forward Mach number by decreasing the tip Mach number through operation at increasing values of blade angle.
5. The general form of the changes in thrust and power coefficients was similar to the changes in airfoil lift coefficient with changes of Mach number.
6. Losses in propeller efficiency due to compressibility effects decreased with increase of blade width.
7. An increase of blade solidity from 0.03 to 0.045 permitted an increase in critical tip Mach number of 0.03.
8. The range of power disk loading for high efficiency decreased with increase of forward speed as a consequence of compressibility effects. This decrease in range of high efficiency indicated that propeller designs for high-speed aircraft may be critical and that it will likely prove necessary to design propellers to fit specific applications.
9. At constant power coefficient, an increase of solidity improved the efficiency for climb and high-speed conditions.

LANGLEY MEMORIAL AERONAUTICAL LABORATORY,
NATIONAL ADVISORY COMMITTEE FOR AERONAUTICS,
LANGLEY FIELD, VA., *January 22, 1944.*

## REFERENCES

1. Stack, John: Tests of Airfoils Designed to Delay the Compressibility Burble. NACA Rep. 763, 1943.
2. Hartman, Edwin P., and Feldman, Lewis: Aerodynamic Problems in the Design of Efficient Propellers. NACA ACR, Aug. 1942.
3. Becker, John V.: Wind-Tunnel Tests of Air Inlet and Outlet Openings on a Streamline Body. NACA ACR, Nov. 1940.
4. Wenzinger, Carl J.: Wind-Tunnel Investigation of Several Factors Affecting the Performance of a High-Speed Pursuit Airplane with Air-Cooled Radial Engine. NACA ACR, Nov. 1941.
5. Fage, A., Lock, C. N. H., Bateman, H., and Williams, D. H.: Experiments with a Family of Airscrews Including Effect of Tractor and Pusher Bodies. Part II—Experiments on Airscrews with Tractor and Pusher Bodies. R. & M. No. 830, British A.R.C., 1922.
6. Wood, Donald H.: Full-Scale Tests of Metal Propellers at High Tip Speeds. NACA Rep. 375, 1931.
7. Weick, Fred E.: Aircraft Propeller Design. McGraw-Hill Book Co., Inc., 1930.